LUND UNIVERSITY

Feasibility of adaptive SBRT of prostate cancer: Investigating uncertainties in AI-driven and CBCT-guided online adaptive radiotherapy

---

Sevgi Emin

Supervisors:
Lina Andersson, Lucie Calmels, Patrik Sibolt, and David Sjöström

This project was conducted at the Radiotherapy Research Unit,
Department of Oncology, Herlev Hospital

Popular scientific summary in Swedish

Cancer kan drabba vem som helst och kan ha sitt ursprung i många olika områden i kroppen. Antalet nya cancerfall ökar varje år, men vissa typer av cancer har bättre prognos än andra.

Den vanligaste cancertypen i Sverige är prostatacancer och den drabbar framför allt äldre män. Prostatacancer har god prognos och det finns effektiva metoder att helt bota prostatacancer om den behandlas i ett tidigt stadie. Ett sätt att behandla prostatacancer är genom strålbehandling, där prostatan bestrålas vid flera behandlingstillfällen genom en strålkanon. Vanligtvis behöver patienten få sin behandling under ca 39 tillfällen, vilka sträcker sig över en period av 8 veckor. Det är möjligt att förkorta behandlingen till enbart fem tillfällen genom att öka mängden strålning patienten får vid varje tillfälle.

Strålbehandling är en effektiv metod att behandla prostatacancer, men kan leda till biverkningar om man bestrålar de friska organen kring prostatan såsom ändtarmen och urinblåsan. En röntgenbild av patienten tas vid varje behandlingstillfälle för att kunna se hur prostatan ligger relativt strålkanonen och kunna rikta strålningen korrekt, varefter patientens position justeras för att överensstämma med positionen på datortomografibilderna som användes för planeringen av strålbehandlingen. Att ändra patientens position är dock inte alltid tillräckligt för att återskapa prostatans position som i planeringssituationen. Kroppen ändras hela tiden, och kan se olika ut vid de olika behandlingstillfällena. Den planerade behandlingen kan passa väl vissa dagar och betydligt sämre andra dagar. Så varför anpassas inte behandlingen till patienten istället för att anpassa patienten till behandlingen? Hittills har de tekniska förutsättningarna inte funnits tillhands, men nyligen blev ny teknologi tillgänglig som möjliggör att en ny behandlingsplan skapas för patienten vid varje enskilt behandlingstillfälle inom en rimlig tidsram. Den här typen av behandling kallas för online adaptiv och används för att ge en behandling som passar patientens kropp just den dagen.

I detta projekt undersöktes om online adaptiv strålbehandling kan användas för att behandla prostatacancer med färre behandlingstillfällen än traditionellt genom ökad bestrålning vid varje tillfälle, utan att otillbörligen skada omkringliggande organ. Det utvärderades hur bra metoden är på att ge den ordinerade behandlingsdosen till prostatan, där cancern fanns, och hur mycket de omkringliggande friska organen påverkades.

Projektets resultat pekar mot att online adaptiv strålbehandling har fördelar när det kommer till mängden bestrålning prostatan får. Det kunde inte påvisas stora förändringar i bestrålningen av de friska organen, jämfört med en traditionell strålbehandling där planen inte anpassades vid varje behandlingstillfälle. Möjligheten att minska denna bestrålning kommer att undersökas vidare i framtida studier.

Abstract

Purpose: Recent developments in external radiotherapy and its utilization with artificial intelligence (AI) enables advanced treatment plans for a range of different disease sites. By adapting to the anatomy of the day, target coverage can be ensured while sparing more healthy tissue. The purpose of this project was to study the feasibility and benefits of daily cone beam computed tomography (CBCT)-based online adaptive radiotherapy (oART) for localised prostate cancer using the Varian Ethos™ treatment planning system (TPS). The possibility of increasing dose per fraction, while sparing organs at risk (OAR), was investigated.

Materials and method: Online adaptive stereotactic body radiotherapy (SBRT) (5 x 7.25 Gy/fr) was simulated in a pre-clinical release of the Ethos TPS for 10 prostate cancer patients using retrospective data. The system used AI-generated influencers for structure-guided or elastic deformation of targets and OAR from the reference situation on the planning computed tomography (CT) image to the online acquired CBCT images. For a localised prostate cancer treatment, the influencers used were bladder, rectum, and prostate, as defined on CT, while the prostate target was defined on magnetic resonance (MR) images. Based on the propagated target, the system generated two plans: scheduled and adapted. The scheduled plan was re-calculated based on the anatomy of the day, whilst the adapted plan was both re-optimised. The influencer editing required to achieve accurate target propagation was evaluated. The absorbed dose to clinical target volume (CTV), planning target volume (PTV), and rectum for the scheduled and adapted plans was compared. A 5 mm isotropic CTV-PTV margin was used.

Results: The AI could propagate an MR-defined prostate target based on a CT-defined prostate influencer. However, of all propagated targets, 69.4% were larger in volume than the target on the planning CT (reference target). The propagated target position with respect to the reference target was satisfactory, where only 10% of all propagated targets were extending outside the reference PTV. The average absolute difference in position and its standard deviation were: 1.19 ± 1.14 mm in the sagittal plane, 1.90 ± 1.66 mm in frontal, and 1.06 ± 1.26 mm in transversal planes. A statistically significant difference was seen between scheduled and adapted plans ($n=49$) in the absorbed dose to 99% of CTV volume ($p=0.00$) and to 99% of PTV volume ($p=0.00$). There was no significant difference in the maximum absorbed dose to the rectum ($p=0.36$) , in the rectum volume that received 28 Gy ($p=0.67$) and the rectum volume that received 32 Gy ($p=0.10$).

Conclusions: The Varian Ethos TPS was observed to deform an MR-defined prostate target when CT-defined prostate was used as influencer. The propagated target volume differed from the reference target, but its position was accurate. The system could be advantageous for daily online adapted SBRT prostate treatments with sufficient CTV and PTV coverage. The reduction of toxicity to rectum needs further investigation.

Acknowledgments

I would like to start with thanking my encouraging supervisors:

Lina Andersson: thank you for all the help throughout this project and for your positive energy. It was always fun to discuss things with you and you always gave me valuable feedback and ideas to solve problems.

Lucie Calmels: thank you for always helping me out whenever I had a problem with Ethos or Eclipse. You were always available to support me in whatever problem I encountered.

David Sjöström: thank you for being so enthusiastic and creative. The discussions with you challenged my way of thinking and helped me learn even more during this project.

Patrik Sibolt: thank you for your feedback, support and all useful ideas.

I would also like to thank my fellow classmate and friend **Daria**. You made this whole period much more fun and helped me sort out my thoughts whenever I was struggling.

Contents

List of abbreviations

AI artificial intelligence

AP anterior-posterior

CBCT cone beam computed tomography

CC cranio-caudal

CT computed tomography

CTV clinical target volume

DSC dice similarity coefficient

EBRT external beam radiotherapy

GTV gross tumour volume

IMRT intensity-modulated radiotherapy

LR left-right

MRI magnetic resonance imaging

OAR organs at risk

oART Online adaptive radiotherapy

PTV planning target volume

QA quality assurance

SBRT stereotactic body radiotherapy

sCT synthetic CT

TPS treatment planning system

VMAT volumetric modulated arc therapy

Chapter 1

Introduction

Cancer is a generic term for diverse diseases that can be generated from almost every cell type in the body. It is caused by a cell mutation that leads to an uncontrollable division and spreading to surrounding tissues. Each cell type gives rise to a certain form of cancer and multiple cancer forms can develop from each cell type. This development depends on factors such as cell location and genetic aberrations [1].

One cancer type is prostate cancer, which has its origin in the prostate gland. It is the most common type of malignancy in men, accounting for approximately a third of all male cancer occurrences in Sweden [2]. A commonly used treatment method for prostate cancer is external beam radiotherapy (EBRT), where ionising radiation is applied to the tumour using an external source. Depending on the properties of the tumour and the patient's condition, the patient gets prescribed a certain radiation dose given in smaller fractions. Research shows that prostate cancer benefits from treatment dose escalation, applied with high dose per fraction in few fractions [3]. This type of treatment is referred to as stereotactic body radiotherapy (SBRT).

No increase in late toxicity has been observed after SBRT treatments compared to treatments with lower fraction dose [4], [5]. As the SBRT dose per fraction is very high, the knowledge of the target and the organs at risk (OAR) position at each fraction is crucial. Online adaptive radiotherapy (oART), where the treatment is adapted to the anatomy of the day, can provide a benefit in the treatment of prostrate cancer with SBRT.

1.1 Project aim

The overall purpose of this project was to study the feasibility and benefits of daily cone beam computed tomography (CBCT)-based online adaptive SBRT of prostate cancer using the Ethos™ treatment planning system (TPS) (Varian Medical systems, Palo Alto, CA, USA). This was done by:

1. developing a method to investigate the uncertainties in the online adaptive process for prostate cancer,
2. examining the possibility to increase dose per fraction while sparing OAR.

Chapter 2

Theoretical Background

2.1 Prostate anatomy and physiology

The prostate gland is a part of the male reproductive system and its function is essential for male fertility.

It secretes a slightly acidic fluid, which contains elements that control the ejaculation process and regulate proteins from other glands that activate sperm maturation [6].

As can be seen in Figure 2.1, the prostate gland is located anterior to the rectum, inferior to the urinary bladder and seminal vesicles and it surrounds the proximal urethra. It has a conical shape and is on average 20 g for a male adult. The prostate gland is composed of glandular and stromal elements and is wrapped by a pseudocapsule. The prostate consists of 3 different zones called the central zone, transition zone and peripheral zone. The peripheral zone is the largest one and is the most common location for carcinoma, chronic prostatitis, and post-inflammatory atrophy [7].

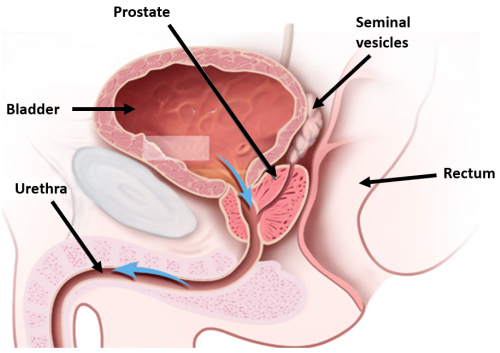

Figure 2.1: Diagram of prostate with respective positions of bladder, rectum and seminal vesicles. *Source by Wikimedia Commons distributed under a CC-BY 4.0 license:* `https://commons.wikimedia.org/wiki/File:BPH_blank.png`

2.1.1 Prostate cancer

There is a strong correlation between age and prostate cancer incidence and mortality rates, where the risk is the highest for men above 65 years old. The prognosis for prostate cancer is good and it can be completely cured if it is treated at an early stage [8].

The most common methods used for treating prostate cancer are:

- **active surveillance/active monitoring:** an immediate curative therapy strategy is not employed, instead the patient is observed while applying palliative care,

- **radical prostatectomy:** the prostate gland and the surrounding tissues (such as seminal vesicles and close by lymph nodes) are surgically removed,
- **EBRT:** ionising radiation from an external source is applied to the prostate from outside the body,
- **brachytherapy:** sealed radioactive sources are implanted inside the prostate,
- **hormonal therapy:** used for various reasons in the management of different stages of prostate cancer, for example lowering testosterone levels,
- **chemotherapy:** a drug based treatment method used to target fast growing cells in the body,
- **immunotherapy:** a treatment method that uses the immune system to target cancer cells.

The choice of treatment method is based on the stage of the cancer and the patient's health condition. The treatment is often a combination of the methods mentioned above [9].

2.2 External beam radiotherapy of prostate cancer

EBRT is one of the most commonly used methods for treating prostate cancer. The method takes advantage of ionising radiation to externally deliver a prescribed radiation dose to a target volume as accurately as possible. The ionising radiation damages cancer cells through radiolysis (splitting of DNA molecules due to radiation). This affects the functions of the cell, leading to cell death. In this way, the development of the tumour can be slowed down or diminished [10].

The ionising radiation used for EBRT is produced using a linear accelerator (linac), which makes it possible to aim the beam towards the patient from different angles and focus the delivered radiation dose to the tumour, while allowing for sparing of surrounding normal tissue or OAR. In a linac, electrons are accelerated to produce a high energy photon beam, which is later shaped and focused in the linac treatment head to fit the treatment area. The energy deposited by those photons to the tissue per unit mass is defined as absorbed dose and is measured in the unit gray (Gy) [11].

Usually a high radiation dose is prescribed and it is delivered in smaller parts (fractions) over a longer period of time. Fractionation is used instead of a single high dose to achieve better tumour control for the same level of normal tissue toxicity. This is due to the fact that the time between the fractions provides the time needed for normal cells to repair sublethal damage and repopulate. At the same time, this intra-fractional time increases the damage to tumour cells due to re-oxygenation and re-assortment of cells into radiosensitive phases of the cell cycle between the fractions [12].

2.2.1 Stereotactic body radiotherapy (SBRT) of prostate cancer

The conventional prescribed radiation dose for localised prostate cancer is 78 - 80 Gy and usually delivered in 1.8- 2 Gy/fraction and 5 fractions/week. The relatively small dose per fraction leads to a longer treatment duration, which can be logistically demanding both for the patient and the hospital. Research shows that prostate cancer has a low α/β value, which is a measure of fractionation sensitivity of cells [13]. This implies that prostate cancer cells are more sensitive to high doses per fraction. This high dose can be delivered by brachytherapy or EBRT with high fractionation dose. The advantage of using EBRT is that steep dose gradients can be achieved using already existing equipment and risks related to the surgical procedure in brachytherapy can be avoided [14].

Depending on the fractionation dose, this type of radiotherapy can be referred to as hypo-fractionated (2.2- 4 Gy/fraction) or SBRT treatment (higher than 4 Gy/fraction) [14]. Many studies have been conducted to study the effect of SBRT on prostate cancer treatment and reviewed in an article by *Beckta et.al.* [14]. The results showed freedom from biochemical recurrence rate of 90 % to 100 % for low and intermediate risk patients. The rate was observed to be lower for high-risk patients (70 %). SBRT also had $\geq$ *grade 2* gastrointestinal and genitourinary toxicity values comparable to conventional and hypo-fractionated treatments [14]. The gastrointestinal toxicity in SBRT can be decreased further by using dissolvable, biocompatible hydrogels to temporarily increase the distance between the rectum and the prostate, and hence reduce the dose to the rectum wall [15]. Another benefit with SBRT is the shorter treatment duration, which is more logistically beneficial both for the patient and the hospital. Research shows that SBRT is more cost-effective for hospitals than intensity-modulated radiotherapy (IMRT) treatments [16].

2.2.2 Prostate volume change during external beam radiotherapy

Treating the prostate with ionising radiation can lead to changes in the gland's morphology. According to studies by *King et. al.* and *Nichol et.al.*, a slight increase in the prostate volume has been observed in the beginning of conventionally fractionated treatments [17], [18]. During the course of the treatment, the prostate deformed and shrank below its baseline volume [17]. Migration of fiducial markers, inserted into the prostate prior to the treatment, was also observed [18].

For an SBRT treatment, another study by *Gunnlaugsson et. al.* showed a 14% increase in the average prostate volume in the middle of the treatment course [19]. The prostate remained swelled during the whole treatment. The enlargement was more prominent in the anterior-posterior and cranio-caudal directions.

2.2.3 Treatment planning

During EBRT both the tumour and surrounding normal tissues are irradiated. A therapeutic gain is obtained when the amount of absorbed dose to the tumour is greater than the dose to the normal tissues or OAR. In order to achieve this, it is important to have good knowledge of the tumour's properties, such as its precise three dimensional location in the body and the tumour's inter- and intra-fractional change.

When defining the volume to be irradiated during EBRT, the current clinical practice is to use both computed tomography (CT) and magnetic resonance imaging (MRI). MRI is used for its superior soft tissue contrast and is favorable for defining organs, such as the prostate. CT, on the other hand, is used for dose calculations. Target and some OAR are delineated on the MR-image and transferred to the planning CT-image via rigid image registration, usually based on fiducial markers implanted into the prostate.

After the target and OAR are defined, there are different treatment methods available. Often used methods for prostate cancer treatment are IMRT and volumetric modulated arc therapy (VMAT) . In IMRT, the radiation is delivered using sub-beams with different intensities or dimensions from each fixed beam direction. Radiation with VMAT is delivered from a large number of beam directions in an arc trajectory. The beam intensities are uniform and the size and number of arcs can be adjusted. VMAT is often preferred over IMRT due to its improved delivery efficiency [20].

The treatment planning of IMRT and VMAT plans is based on an automated iterative optimisation using defined dose-volume constraints and mathematical objective functions. These guide the resulting optimal beam geometry and intensity. The dose-volume constraints are used to minimise the absorbed dose to normal tissues and OAR, while optimising target dose homogeneity and coverage [21].

CTV–PTV margins

Another important concept in EBRT planning is clinical target volume (CTV) and planning target volume (PTV). The CTV is defined as the volume containing the gross tumour volume (GTV) and/or subclinical microscopic malignant lesion, that leads to a risk of malignancy occurrence and therefore needs to be taken into account while treating. The PTV on the other hand, is a geometrical concept that is used for treatment planning and evaluation. The PTV surrounds the CTV with a certain margin that takes uncertainties in the EBRT process into account [21]. These uncertainties are categorised in systematic and random errors. During treatment preparation, systematic errors can be introduced due to uncertainties in imaging, target delineation, treatment planning and delivery. During treatment delivery both random and systematic errors can occur from uncertainties in patient setup and target motion. These systematic and random errors can be both inter- and intra-fractional errors. Inter-fractional errors occur from one treatment session to the other, while intra-fractional

errors occur during the treatment session [22].

An often used formula for CTV– PTV margin calculation is $2.5\Sigma + 0.7\sigma$, where Σ represents the standard deviation of the systematic error and σ represents the standard deviation of the random error [23]. A study by *Levin-Epstein et.al.* estimated the contribution from inter-fractional errors for prostate patients to be on average -0.03 ± 0.30 cm, -0.06 ± 0.43 cm, and -0.06 ± 0.45 cm in the left-right, cranio-caudal, and anterior-posterior directions respectively [22]. Intra-fractional prostate motion was measured to be <3 mm during an EBRT treatment and depended mostly on the rectal filling [24], [25]. The CTV– PTV margins proposed by literature for a prostate treatment are 5 mm, when fiducial markers are used for positioning, with a possibility to decrease to 3 mm if real-time tracking methods are incorporated [26]. Institutional investigation (not published) at Herlev Hospital shows similar results. The margins are dependent on e.g. patient fixation and staff experience and optimally the CTV– PTV margin should be investigated and determined for each institution.

The CTV– PTV margin is an important factor in the absorbed dose distribution due to the steep dose gradients between target and OAR. Too small margins can lead to underdosage of target, whilst too large margins can lead to increased dose to normal tissue and OAR [21]. A method to reduce margins is to adapt the treated volume at each fraction, based on the anatomy of the day. By doing that, some uncertainties, e.g. due to inter-fractional variations in the anatomy, can be reduced. Uncertainties can be introduced from the oART workflow as well and need to be taken into account in the margin size. These uncertainties could be due to target and OAR propagation, and synthetic CT (sCT), used for dose calculation while online adapting.

2.2.4 Treatment delivery

The on-couch delivery of the treatment plan can be done in different ways: conventionally or by online adaptation. In the sections below the conventional and online adaptive treatment workflow for prostate cancer are described.

Conventional workflow

In a conventional EBRT workflow, a treatment plan is prepared for a patient using planing CT- and MR- images. This plan is applied at every fraction and in cases of extreme changes in patient anatomy, re-planning might be necessary.

Since a single treatment plan is used, it is important to verify that the target is positioned identically at every treatment fraction. This is necessary to make sure that the prescribed radiation dose is delivered to the target and normal tissue is spared. In the case of prostate cancer, the gland is surrounded by sensitive and vitals organs such as the rectum, bladder

and the reproductive system. To be able to replicate the treatment at each fraction, fiducial markers, inserted into the prostate, are used to localise and correct the prostate position prior to treatment delivery. This is done by an automatic fiducial marker match between the CBCT and planning CT images and calculating the necessary correction to the patient's position [10]. These fiducial markers are also used for other purposes, such as MR- and CT- image matching at the treatment planning stage or for monitoring the intra-fractional motion of the prostate during the treatment.

In Figure 2.2, the workflow for conventional radiotherapy is shown. In the first step of the treatment, a CBCT image of the patient is taken. Thereafter, the patient position is adjusted by comparing the current position of the fiducial markers in the CBCT image to the original position in the planning CT images. Once the on-couch position is adjusted, the patient is treated. This method of treatment assumes that the body is a static system and does not take anatomical changes into account.

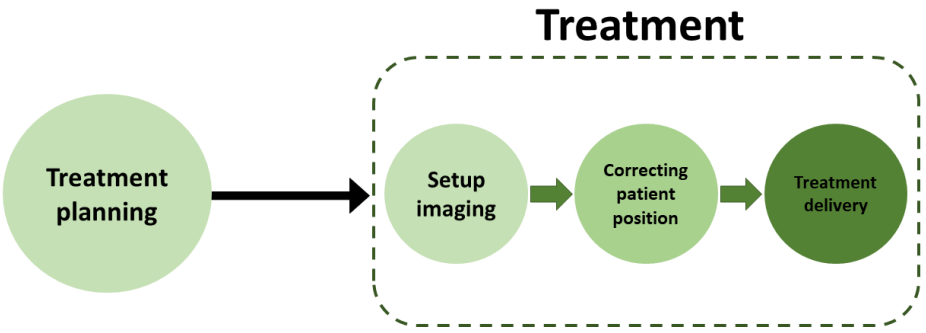

Figure 2.2: Different steps in the conventional radiotherapy workflow.

Online adaptive radiotherapy workflow

In comparison to the conventional workflow, the initial treatment planning for CBCT based daily oART using the Ethos™ TPS (Varian Medical systems, Palo Alto, CA) is mostly automated and requires minimal user input. In the first step of the planning process, the user selects a template for the anatomical region and defines the target and OAR volumes and their constraints. These constraints are ordered based on their priority. The dose-volume constraints and their priority are referred to as the planning directives and are later used as the basis for the automatic generation of all future plans for this treatment, generated both offline and online. Based on the planning directives, the Intelligent Optimization Engine, an algorithm managing plan optimisation, automatically generates several IMRT and VMAT plans with different beam geometries. A comparison of the plans is presented and the user selects one of these as the reference plan [27].

In an oART workflow for prostate cancer the patient's position does not need to be adjusted based on a fiducial marker match, as the plan is re-optimised for the current target position. The workflow for daily oART is shown in Figure 2.3. The first step, acquisition of CBCT images, is identical to the one in the conventional workflow. The CBCT image is used for automatic artificial intelligence (AI)-driven segmentation of some structures in the closest proximity to the target (for some cases also the target), referred to as influencers. These influencers are pre-defined by the system, based on the anatomical site, and guide both target- and OAR deformation [27].

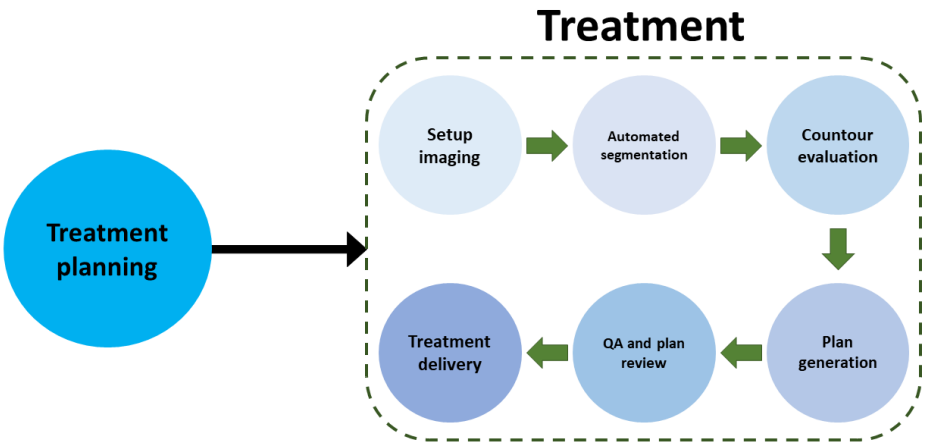

Figure 2.3: Different steps in the online adaptive radiotherapy workflow.

The next step in the oART workflow is online evaluation and adjustment of influencer contours by users. Once the influencer evaluation is completed and approved, a structure guided or elastic deformation algorithm begins propagating the CTV from the planning CT to the CBCT, and the PTV is derived from the CTV. Such as the case with the influencers, the propagated target contours need to be evaluated and if necessary manually adjusted.

Based on new target and OAR structures, two plans are generated: scheduled and adapted plan. The dose distribution is re-calculated for the scheduled plan and re-optimised by the Intelligent Optimization Engine for the adapted plan. The system does a rigid registration between the planning CT and CBCT to maximise target coverage for the scheduled plan. Both scheduled and adapted plans use the same beam geometry, objectives and constraints as the reference plan. For the dose calculation a sCT image is generated by deforming the planning CT to the daily CBCT. The user evaluates both plans and selects the plan that is most optimal in relation to the constraints. Before treatment delivery is initiated, an independent dose calculation of the selected plan is performed using Mobius3D (v2.2).

Chapter 3

Materials and Methods

3.1 Investigating uncertainties in oART of prostate cancer

3.1.1 Influencers for daily oART of prostate cancer

The influencers (described in Section 2.2.4) for a prostate treatment are: bladder, rectum, prostate and seminal vesicles. The TPS offers the user the possibility to deselect these influencers according to their usefulness.

As a first step in this project, the effect of each influencer on the target propagation was evaluated in a pre-clinical version of the TPS and treatment console (emulator) using retrospective data for two patients with localised prostate cancer: *Patient A* and *B*. All influencers were defined on the planning CT-images, while the target was defined on MR-images and later transferred to the CT-images by fiducial marker based rigid image registration.

When studying the effect of each influencer on propagated target, the MR-defined prostate, referred to here as the reference target, acted as ground truth. The focus in the project was a prostate only treatment. The following method was used to study the effects of influencers on target propagation:

1. One of the influencers was excluded (not defined) in the treatment plan and the remaining influencers were handled as usual.
2. In the next trial, the influencer that was previously excluded was defined. The size and location of the propagated target was compared with the propagated target from *step 1*. The size of the reference target was taken into account.
3. Evaluation of results:
    - An influencer was considered to be important for target propagation if the propagated target location and shape did not correspond with the reference target after that specific influencer was excluded. A target was considered to do not correspond with the reference target, if it e.g. overlapped with the bladder and the rectum in a way that was not observed in the reference situation or if it was enlarged in a direction that was not present in the reference target.

- An influencer was considered insignificant if the target propagation was not affected by its exclusion.

The next step was to study how accurate the AI-algorithm was at segmenting the influencers to investigate the risk of a systematic uncertainty in this step of the workflow. This was done by studying the shape and size of the influencers, automatically generated by the AI on the CBCT, without applying any adjustments. The retrospective data from the same patients was used for these tests. The CBCT-images from a fraction in the beginning, middle and end of the treatment were selected to obtain a variety in the patients' anatomy. More information about the patients can be found in Appendix A, Table A.1.

3.1.2 Target propagation

After influencer propagation and evaluation, the next step in the daily oART workflow is target propagation. This is an automatic process, where the targets are deformed by either elastic or structure-guided deformation depending on their overlap with the influencers. The amount of influencer editing necessary for accurate target propagation was tested to investigate the possibility for shortening the time spent on the influencer evaluation step in the oART workflow. Simultaneously, it was also evaluated if an MR-based target could be propagated correctly using a CT-based prostate influencer. Retrospective data for the same patients as in Section 3.1.1 was used.

The workflow used for this evaluation is shown in figure 3.1. In the first step, the influencer that would be focused on was selected. This could also be all the influencers. Thereafter, it was chosen to adjust the AI-defined contours or not. For all influencers or prostate, if the choice was to adjust, there were two different levels of editing tested: moderate and considerable. These levels were defined based on the time spent for the adjustment of influencer contours. For *Patient A*, the considerable editing time was on average 1.60 times longer than the moderate editing time, whilst for *Patient B* this average difference was 1.40 times. The options for bladder, rectum and seminal vesicle influencers were only to edit or not. The effects of these different scenarios on the propagated target were evaluated in terms of position and volume.

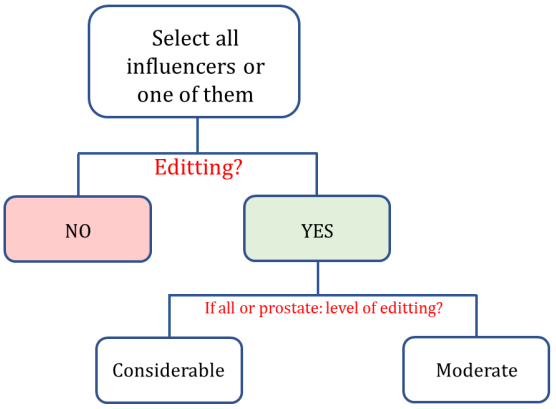

Figure 3.1: Workflow for the determination of the level of influencer adjustment necessary for correct target propagation.

This evaluation was performed in Eclipse™ TPS (v.15.1, Varian medical systems, Palo Alto, CA, USA), where the adapted structure sets from the emulator simulations were imported. To evaluate the propagated target size, its volume was compared to the volume of the MR-defined prostate on the planning CT. This target was used as the ground truth for prostate size and was referred to as the reference target. Afterwards, the structures from the sCT were transferred to the CBCT and a fiducial marker based automatic match was done between the CBCT and the planning CT to study the position of the delineated target with respect to the reference target. After the CBCT-CT image registration, the delineated and the reference target were overlaid as it is schematically shown in figure 3.2. To determine how much these targets overlapped, the dice similarity coefficient (DSC) was obtained from the statistics tool of Eclipse. The DSC is a measure of the spatial overlap between two sets of data (structures in this case). The DSC values can range between 0 and 1, where lower values indicate no spatial overlap and higher values indicate complete overlap [28].

To investigate the spatial position difference between these targets after a fiducial marker match, the residual image slice shift of the overlaid structures was calculated in each direction: left-right (LR), anterior-posterior (AP) and cranio-caudal (CC). This was done by denoting the slice where each structure began and ended (for each target there were 2 values for each direction).

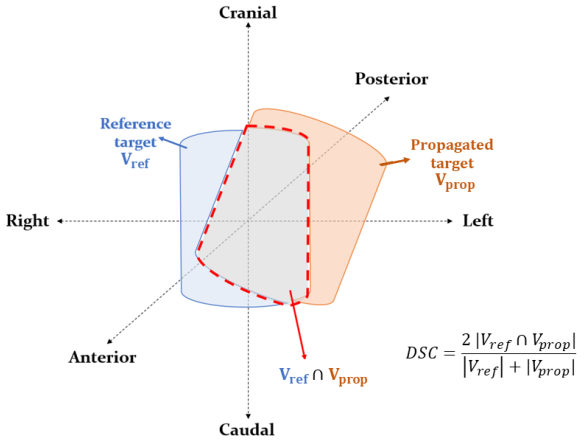

Figure 3.2: Schematic overview of propagated target and reference target, overlaid after a gold seed match. DSC stands for dice similarity coefficient.

Based on the results for target- and OAR propagation for *Patients A* and *B*, the CTV−PTV margin was set to be 5 mm isotropically for the examination of the possibility to increase dose per fraction. The current clinical practice for CTV−PTV margins for localised prostate cancer in Herlev Hospital, Copenhagen are 5 mm in AP and LR directions and 8 mm in

CC direction. It was investigated if these margins were also valid to use for online adaptive SBRT.

3.2 Examination of the possibility to increase dose per fraction

Retrospective data from 10 patients was used to examine the possibility to increase prescribed dose per fraction for SBRT treatment of localised prostate cancer. All patients were previously treated using different fractionation schemes. More information can be found in Appendix A, Table A.1.

To study the dose distribution from an online adapted SBRT, the treatment planning for these test patients was done in the pre-clinical version of the Ethos TPS. The TPS automatically generated 3 IMRT plans with either 7, 9 and 12 fields. The plan that was the most optimal in relation to the constraints was chosen for each patient. This plan was referred to as the reference plan.

The treatment planning constraints are described in Section 3.2.1. Once the treatment plans were approved, the treatments were simulated in the emulator.

3.2.1 Treatment plan

The treatment planning constraints used for the simulations in this project were based on the constraints used for MR-guided adaptive radiotherapy for localised prostate cancer at the Amsterdam University medical center [29]. They are specified in Table 3.1. The prescribed fractionation scheme for the SBRT treatment was 7.25 Gy/fraction in 5 fractions.

The highest priority in the treatment planning was given to the CTV constraints and was followed by the constraint for maximum dose to rectum. Underdosage of PTV was accepted, since it was an online adapted SBRT treatment and the function of the PTV was mostly to compensate for intra-fractional movements of CTV. All values were normalised to the mean dose to CTV.

The constraint for absorbed dose to CTV was set very strict to be able to push the calculation algorithm to increase target coverage.

Table 3.1: Dose constraints for treatment planning of SBRT of localised prostate cancer, adapted from Amsterdam University medical center.

7.25 Gy/fraction x 5 fractions			
Structure	*Constraint*	*Structure*	*Constraint*
CTV	$D99\% \geq 100.0\%$ $D_{mean} \geq 36.00\,Gy$ $D_{mean} < 36.50\,Gy$	Rectum	$D_{max} \leq 34.00\,Gy$ $V28.00\,Gy \leq 30.0\%$ $V32.00\,Gy \leq 10.0\%$
PTV	$D_{max} \leq 105.0\%$ $D99\% \geq 95.0\%$	Bladder	$D_{mean} \leq 20.00\,Gy$
		Femur head & neck left	$D_{max} \leq 30.00\,Gy$
		Femur head & neck right	$D_{max} \leq 30.00\,Gy$

3.2.2 Dose distribution

A total of 50 SBRT treatment fractions for the patients were simulated in the emulator, generating 50 scheduled and 50 adapted plans. An error occurred in the calculation of one fraction, and it was thus excluded from the results. The fractions from which CBCTs were used for these simulations, can be found in Appendix A, Table A.1. To obtain a variety in the patients' anatomy, fractions from different stages of the patients' treatment were selected.

To compare the absorbed dose distribution for the adapted and scheduled plans, it was evaluated how well each plan fulfilled the dose-volume constraints for CTV, PTV and rectum. The focus was laid on these parameters, since the purpose of the project was to investigate the possibility to increase dose to target and spare rectum.

3.2.3 Statistics

To investigate the difference between the dose distributions for the scheduled and adapted plans, a Wilcoxon signed-rank test was used. A non-parametric test was preferred due to the data not being normally distributed, see Appendix B. The measured dose distributions both for scheduled and adapted plan shared the same calculation geometry, which fulfilled the assumption for a Wilcoxon signed-rank test [30]. All statistical analysis was performed in IBM SPSS Statistics for Windows, Version 26.0.

The null hypothesis (H_0) for the Wilcoxon test was that there was no difference between

the median values of the absorbed dose to the CTV, PTV and rectum for the scheduled and adapted plan. The two-tailed alternate hypothesis (H_1) was that there was a difference between the medians.

The significance level (α) represents the probability of rejecting a correct H_0. For these tests, it was chosen to be 0.05.

To study the variation in target volumes and positions, the standard deviation was used. Standard deviation (σ) is a measure of how much each data point (x) deviates from the mean (μ). For a sample with n number of observations, σ for a sample is calculated using:

$$\sigma = \sqrt{\frac{\sum |x - \mu|^2}{n - 1}}$$

The larger the value of σ is, the more spread out the data is [31].

Chapter 4

Results

4.1 Uncertainties in oART of prostate cancer

4.1.1 Influencer propagation

The results for *Patients A* and *B* show that the AI propagated the rectum and bladder influencers accurately and that they required little editing. The rectum had a tendency of being larger in cranial direction compared to the reference structure on the planning CT. The seminal vesicles and prostate influencers required more editing and were larger in CC direction for the two test patients.

Investigating the effect of each influencer on target propagation showed that excluding the rectum and bladder led to an enlargement of the target. It was found necessary to include prostate as an influencer; when excluding the prostate as an influencer, the target was not propagated properly as this resulted in an overlap between CT-based rectum and MR-based target. Finally, excluding the seminal vesicles for a prostate only treatment did not have an effect on target propagation and in some cases led to an improvement in the volume agreement between reference and propagated targets.

4.1.2 Target propagation

An MR-defined prostate target could be propagated correctly using a CT-based prostate influencer, see Figure C.1 in Appendix C. The volume difference in percentage between the propagated and reference target for different amounts of influencer editing is shown in Figure 4.1 for *Patients A* and *B*. All differences were negative, implying that the propagated targets were larger than the reference target.

As it can be seen in Figure 4.1, there was a better volume agreement between reference and propagated target when all influencers were edited moderately or considerably and when only the prostate influencer was edited moderately or considerably. For these cases, the average, maximum and minimum volume differences for each fraction were calculated and are shown in Table 4.1. The average difference was the smallest for fraction 1, increased for fraction 11 and decreased again for fraction 21. This trend was also observed for the cases where there was not a good volume agreement between reference and propagated targets. The volume differences were larger for *Patient B*.

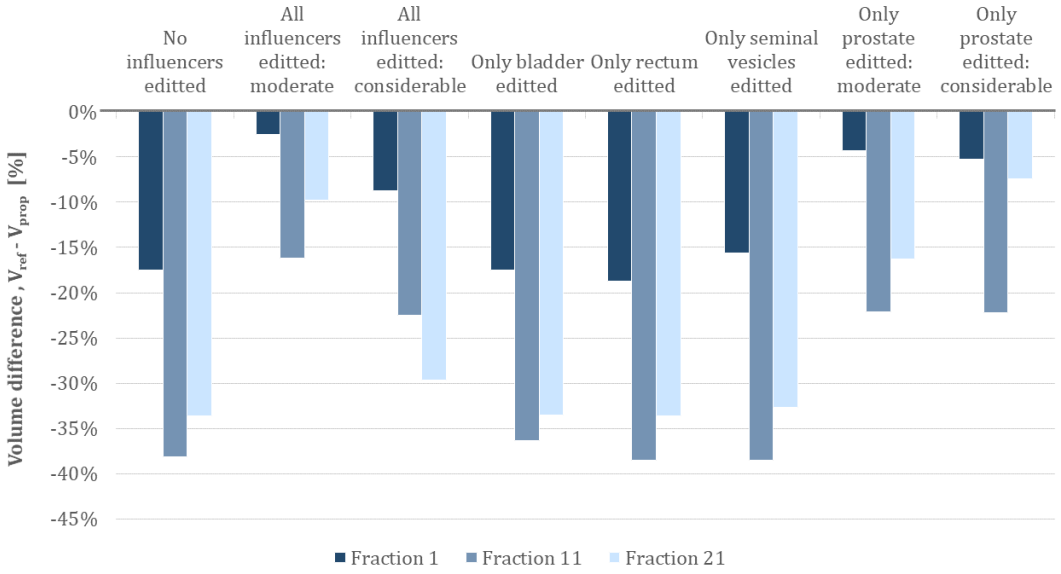

(a) Results for Patient A.

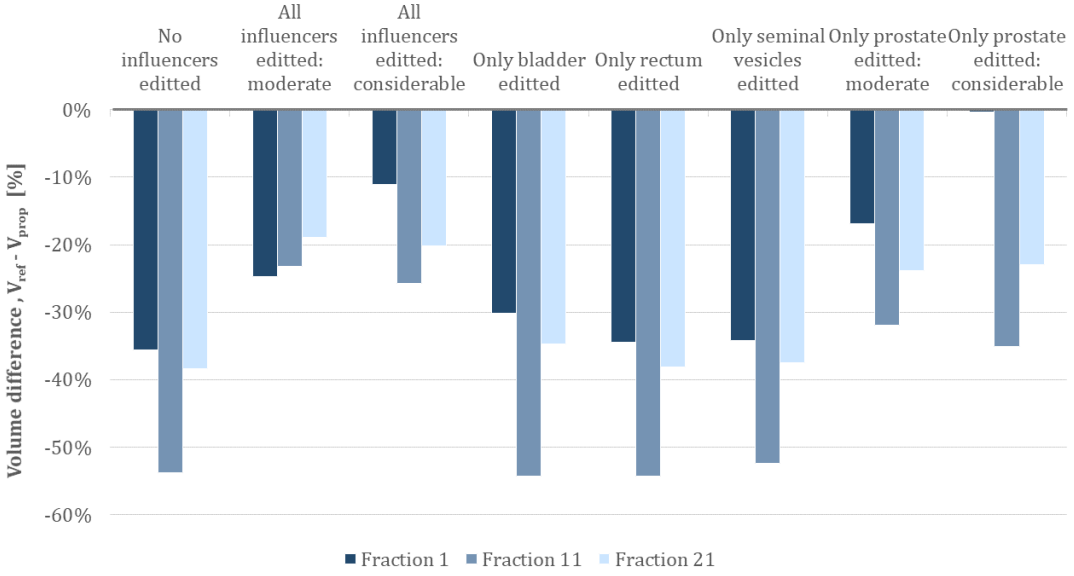

(b) Results for Patient B.

Figure 4.1: Volume difference in percentage between the reference target on the planning CT (V_{ref}) and the propagated targets (V_{prop}) for different amount of influencer editing.

Table 4.1: Average, maximum and minimum volume differences between reference and propagated targets when all influencers were edited moderately and considerably and when only the prostate was edited moderately and considerably.

	Patient A			*Patient B*		
Fraction	**1**	**11**	**21**	**1**	**11**	**21**
Average	-5%	-21%	-16%	-13%	-29%	-21%
Max	-9%	-22%	-30%	-25%	-35%	-24%
Min	-3%	-16%	-7%	0%	-23%	-19%

The DSC for *Patient A* ranged from 0.81 to 0.89 and had an average of 0.87 for the cases where there was a better volume agreement between reference target and propagated target. The range for *Patient B* was 0.78 to 0.89, and the average value was 0.85.

The absolute residual slice difference between the propagated and reference target for both patients was on average:

- 0.8 mm (max-min: 0- 2.7 mm) in LR direction,
- 2.1 mm (max-min: 0- 8.0 mm) in AP direction,
- 1.4 mm (max-min: 0- 4.0 mm) in CC direction.

For more detailed data see Figure C.3 in Appendix C.

4.2 Dose distribution of online adaptive SBRT of prostate cancer

4.2.1 Target volume and position

Prior to investigating the dose distributions, the propagated target from the SBRT simulations was evaluated in terms of volume and position with respect to the reference target for *Patients 1-10*. Out of all propagated targets, 69.4 % were larger in volume compared to the reference target, see Figure 4.2, where a negative value indicates a larger propagated target. The maximum volume difference in percentage was -22% (*Patient 4*), and the minimum difference was 0 % (*Patients 8, 9,* and *10*). The largest differences were observed for *Patients 4, 5, 6,* and *7*.

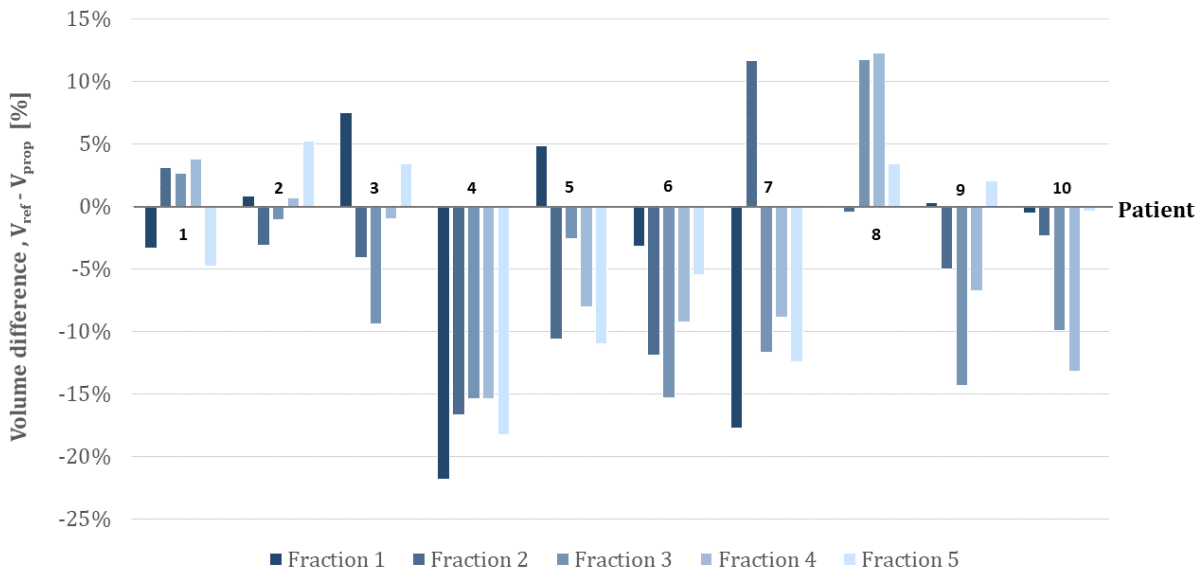

Figure 4.2: Difference between reference target volume (V_{ref}) and propagated target volume (V_{prop}) for all patients over 5 SBRT fractions. The data is presented in percentage [%].

Results from the analysis of the residual slice difference between the propagated and reference target, after an automatic fiducial marker based match, are shown in Figure 4.3. For the majority of the cases, the propagated target was within 5 mm (the reference PTV). Out of all delineated targets (*n=49*), only 10 % were extending outside the reference PTV (4 in *Patient 3* and 1 in *Patient 7*). In Table 4.2, average absolute values and standard deviations of the residual slice differences in each direction can be seen. The largest differences and variances are seen in the AP direction.

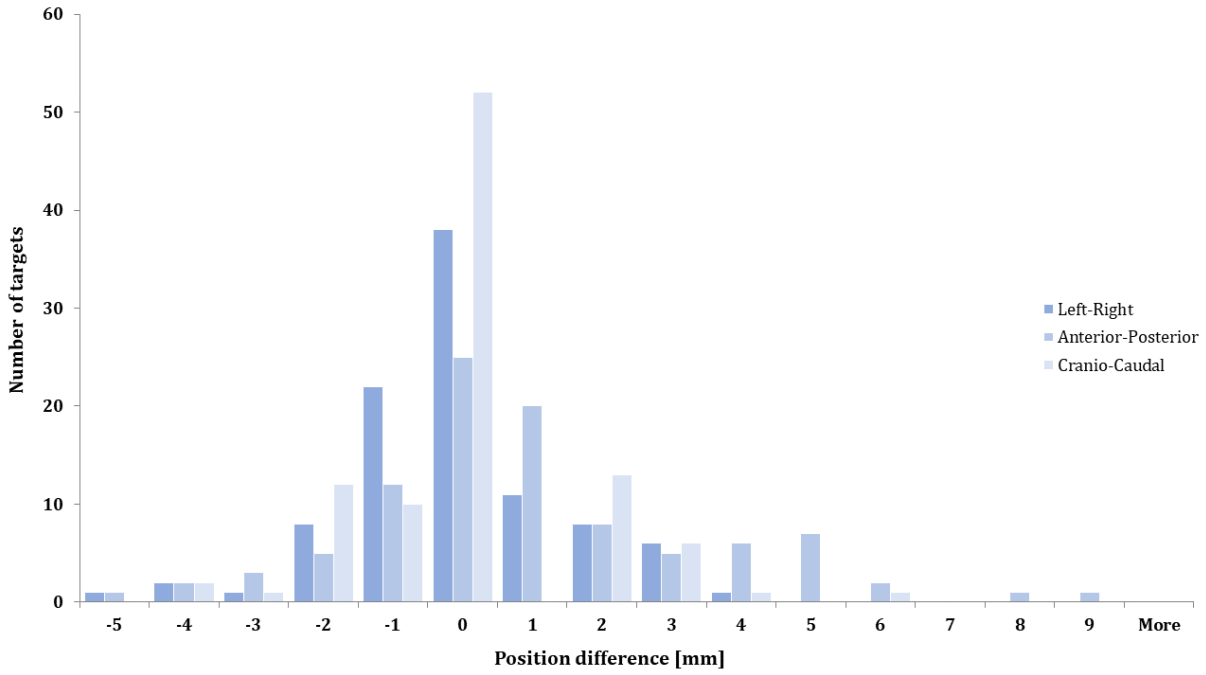

Figure 4.3: Difference in the position of the propagated target with respect to the reference target in the left-right (LR), anterior-posterior (AP) and cranial-caudal (CC) directions. Each target had 2 data points for each direction.

Table 4.2: Average and standard deviations (σ) over absolute values of the data in Figure 4.3.

Direction	Left-Right	Anterior-Posterior	Cranio-Caudal
Average [mm]	1.19	1.90	1.06
σ **[mm]**	1.14	1.66	1.26

In Figure 4.4, the inter-fractional variation in the influencer volumes for each patient is shown. It was evaluated whether these changes had an effect on target propagation. The largest variations in bladder size were seen for *Patient 1* and the largest variations in rectum size were for *Patient 3*. *Patient 7* had large inter-fractional variations in the size of all *OAR*, while patient 6 had the largest variations compared to the planning CT.

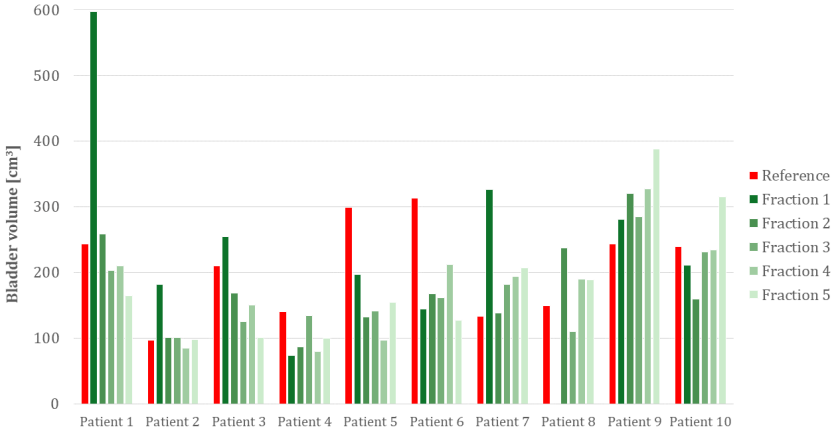

(a) Bladder volume

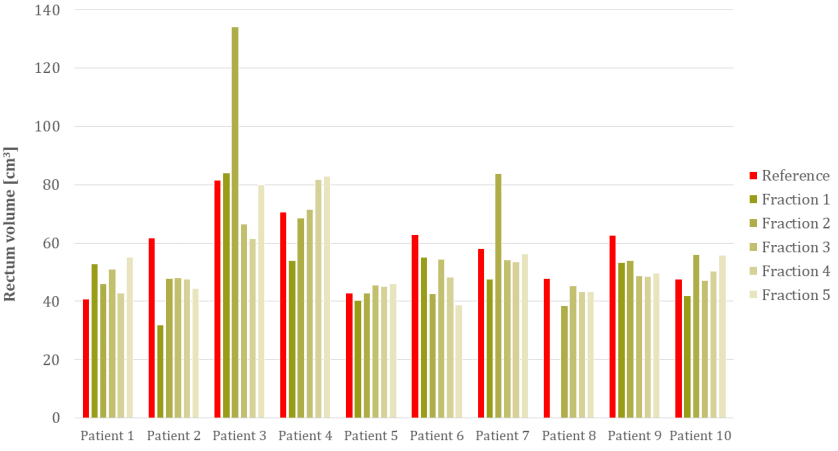

(b) Rectum volume

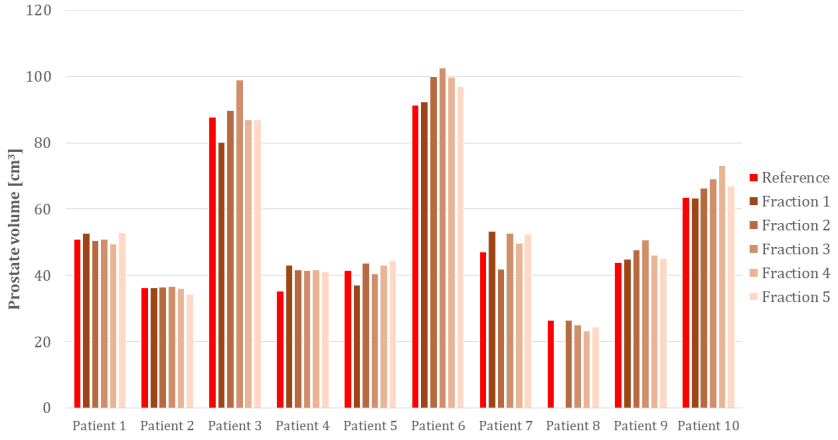

(c) CT-based influencer prostate volume

Figure 4.4: Influencer volumes during 5 SBRT treatment fractions for each patient. The red bars represent the volume of each reference influencer for respective patient on the planning CT-images.

4.2.2 Dose distribution

The absorbed doses to CTV, PTV, rectum and bladder for the adapted and scheduled plan were compared applying the Wilcoxon signed-rank test. The results are shown in Table 4.3. The significance level was set to be 0.05, meaning that there was a statistically significant difference between the adapted and scheduled plans in the absorbed dose to 99% of CTV and 99% of PTV and in the mean dose to CTV. There was no significant difference in the absorbed dose to the rectum and bladder. When a 2 % variation between scheduled and adapted plans was allowed, 69% of all scheduled plans fulfilled the CTV dose-volume constraints as well, accepting PTV underdosage. The rectum dose-volume constraints were acceptable for *55%* of all scheduled plans and out of all scheduled plans, 8% did not fulfill any dose-volume constraints.

Table 4.3: Comparison of absorbed dose to PTV, CTV, rectum, and bladder for scheduled and adapted plans. Average values and the p-value of the Wilcoxon signed-rank test are shown.

Constraint	Plan type	Average	p-value
CTV D99% [%]	Adaptive	98.82	0.00
	Scheduled	96.86	
CTV D_{mean} [Gy]	Adaptive	7.25	0.01
	Scheduled	7.23	
PTV D99% [%]	Adaptive	89.85	0.00
	Scheduled	85.35	
Rectum D_{max} [Gy]	Adaptive	6.68	0.36
	Scheduled	6.71	
Rectum V28Gy [%]	Adaptive	11.12	0.67
	Scheduled	10.94	
Rectum V32Gy [%]	Adaptive	4.18	0.10
	Scheduled	4.75	
Bladder D_{mean} [Gy]	Adaptive	2.03	0.06
	Scheduled	2.11	

In figure 4.5, the variation in the absorbed dose to CTV, PTV and rectum for reference, scheduled and adapted plans for all patients and all fractions is shown. The variation in the absorbed dose and the range were larger for the scheduled plan for all structures. The distribution for the reference and adapted plan were similar and fulfilled the dose-volume constraints more successfully. The adapted plan had several outliers for the absorbed dose to rectum, which belonged to *Patients 1* and *6*, see Figure D.1 in Appendix D.

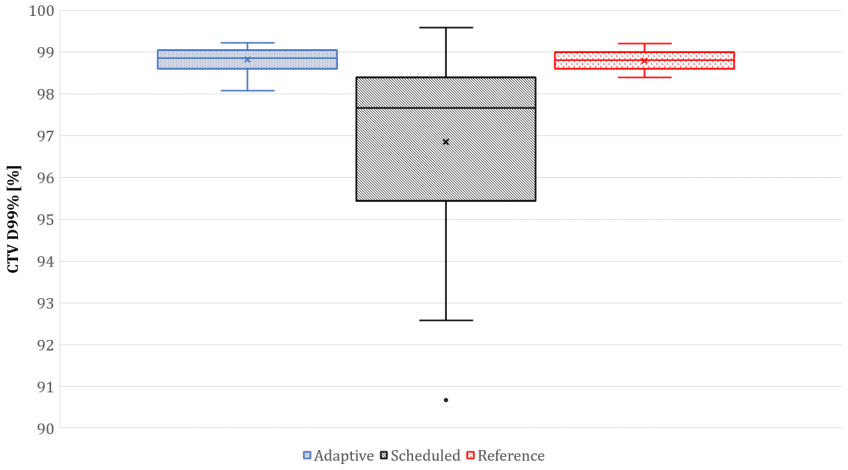

(a) Absorbed dose to the 99% of CTV volume, measured in percentage.

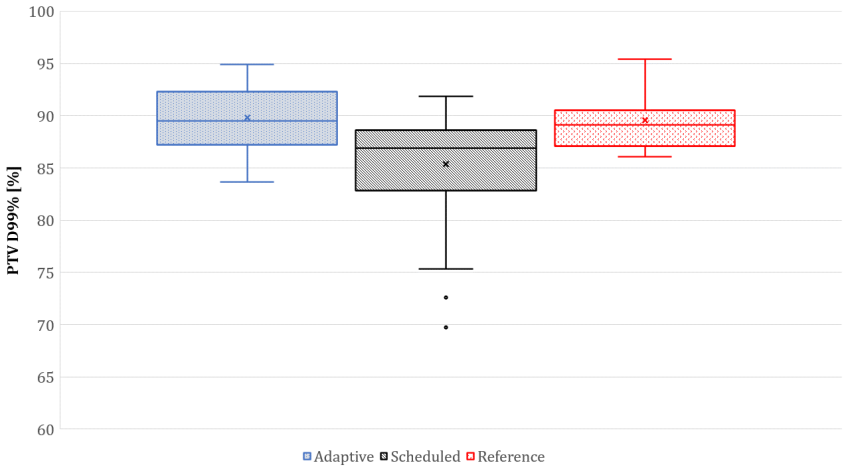

(b) Absorbed dose to the 99% of PTV volume, measured in percentage.

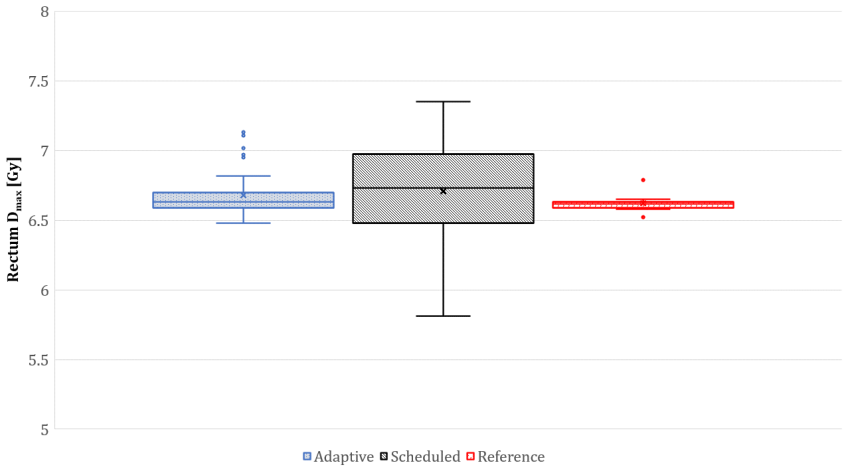

(c) Maximum absorbed dose to the rectum, measured in Gy.

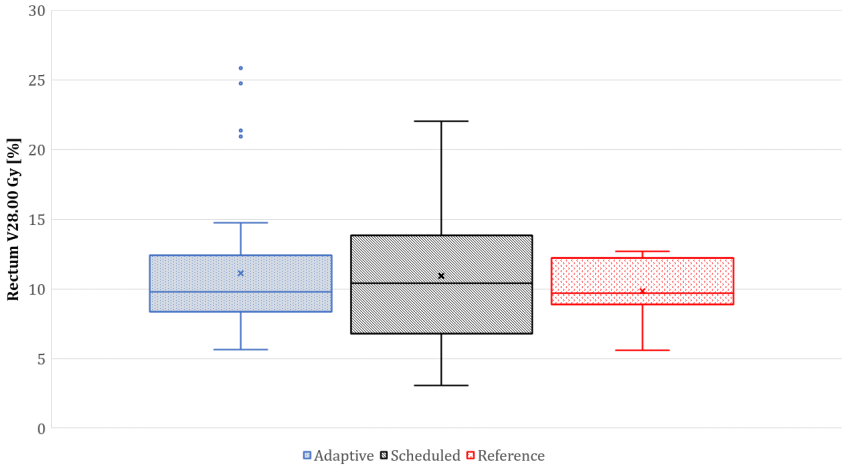

(d) Volume of rectum that receives 28 Gy in absorbed dose, measured in percentage.

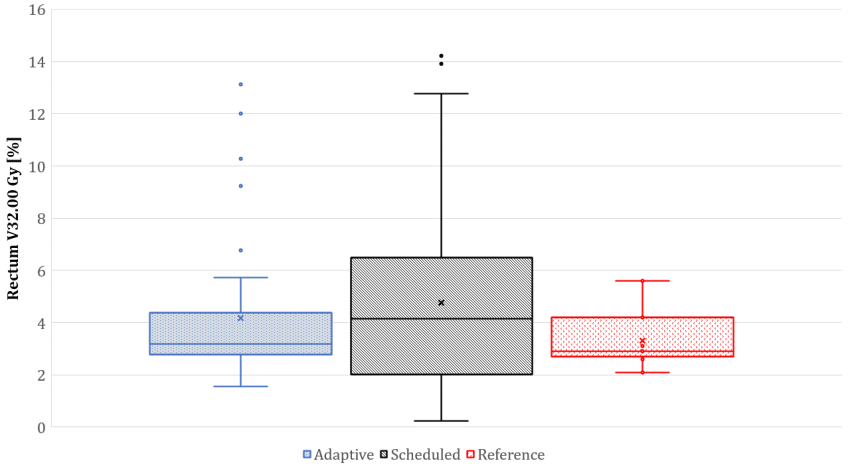

(e) Volume of rectum that receives 32 Gy in absorbed dose, measured in percentage.

Figure 4.5: Box and whisker plots comparing the doses to CTV, PTV and rectum for reference, scheduled and adapted plans for all patients and all fractions. × represents the mean values in each group and ∘ represents an outlier.

A comparison between scheduled and adapted plans for each patient is provided in Appendix D, Figure D.1. This comparison showed that for these 10 patients:

- When it comes to absorbed dose to 99% of CTV, 9 patients benefited from adaptation. The improvement with adapted plan compared to scheduled plan was more than 4% for 3 patients. The mean dose to CTV was improved with adaptation for 5 patients.
- The absorbed dose to 99% of PTV was improved by adaptation for 9 patients, where the increase in dose with adapted compared to scheduled plan was more than 4% for 5 patients, out of which 2 had more than 10% increase in PTV coverage.

- The maximum dose to rectum was reduced for 6 patients via adaptation, where this reduction was more than 3% compared to the scheduled plan.
- The rectum volume that got 28 and 32 Gy was decreased by adaptation for 3 and 6 patients respectively.

Dose-volume histograms (DVH) for two fractions of two separate patients are shown in Figure 4.6. *Patient 1* had a benefit from adaptation during fraction 3, see figure 4.6a. CTV and PTV coverage was improved by adaptation, while absorbed dose to both bladder and rectum was decreased. In Figure 4.6b, DVH for fraction 5 of *Patient 3* is shown. This patient did not have a large reduction in the dose to OAR for the adapted plan and the CTV and PTV coverage was superior for the scheduled plan.

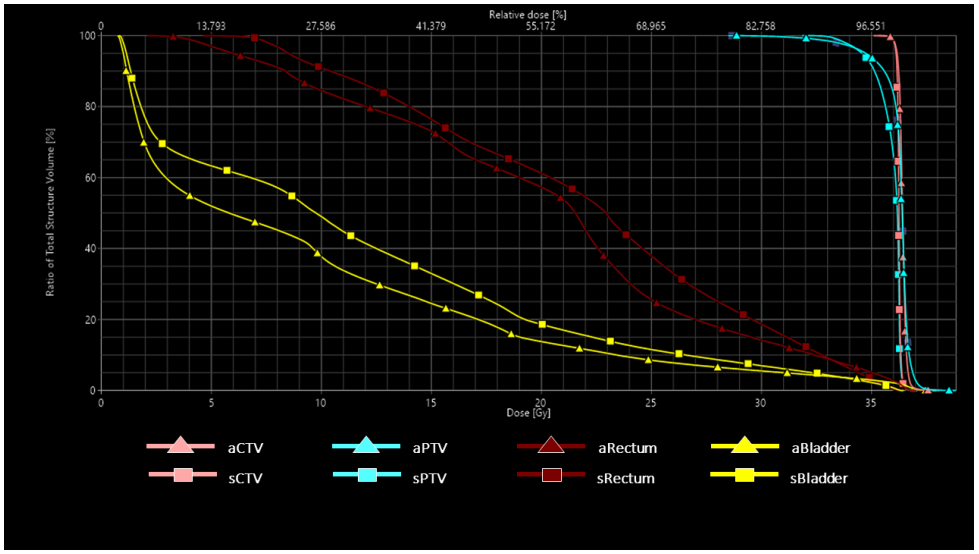

(a) DVH for *Patient 1* treatment fraction 3.

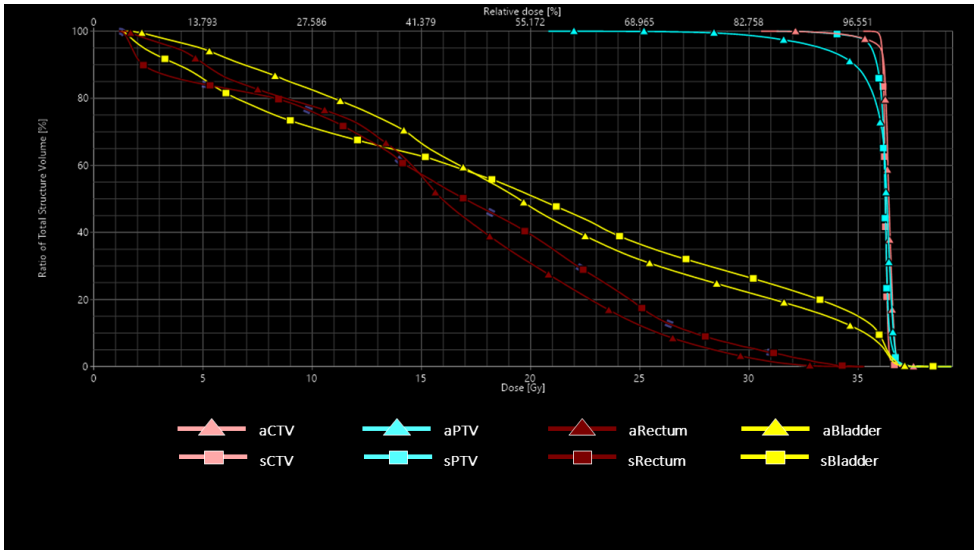

(b) DVH for *Patient 3* treatment fraction 5.

Figure 4.6: Dose-volume histograms (DVH) showing the dose-distribution to CTV, PTV, rectum and bladder for adaptive (*a*) and scheduled plans (*s*) for two different patients. For these fractions, both patients had good position agreement with respect to the reference target.

Chapter 5

Discussion

5.1 Uncertainties in the oART workflow for prostate cancer

The use of a CT- and MRI-based workflow introduces uncertainties both to the conventional and the adaptive workflow. A critical step in using multiple imaging modalities is the target delineation; registration uncertainties up to 2 mm can be introduced when transferring the target from the MR-image to the CT-image via image registration using fiducial markers [32]. These uncertainties could affect the analysis done on the position of the propagated target. The MR-defined target on the planning CT was used as the ground truth both for positioning and volume evaluation. If the match between these two images was not good, the position difference between propagated and reference target could have been affected. The large residual slice differences of propagated target in Figure 4.3, do not necessarily imply that the propagation was inaccurate. The quality of the MR-CT image registration was not evaluated in this study.

The multi-image modality workflow, can furthermore influence the absorbed dose calculation to rectum for an adaptive workflow. In the time between the acquisition of the MR- and CT- images, rectum size changes and when MR-defined target is transferred to the planning CT, the rectum position with respect to target might be inaccurate. This can be caused by a larger rectum, shifting the prostate position, leading to rectum ending up in the CTV/PTV after image registration. Such a case was encountered during the simulations and needed to be corrected. This inaccuracy in position increases the dose to rectum while planning, even if in reality the positioning of these organs in relation to each other is different.

The investigation of influencer and target propagation showed that an MR-based prostate target could be propagated using CT-based influencers. The propagated bladder and rectum influencers required little editing, but the seminal vesicles and prostate influencers often needed a considerable adjustment, mostly in the cranio-caudal direction. This adjustment process could be time consuming due to CBCT image quality and the insufficient soft tissue contrast. In this study, the seminal vesicles were excluded as influencers for a prostate only treatment. Excluding seminal vesicles did not have a negative effect on target propagation and shortened the time spent on influencer evaluation. On average approximately 4 minutes were spent on editing the prostate and 3 minutes on editing the seminal vesicles (Appendix A, Table A.2). Removing the seminal vesicles led to approximately a 17% time reduction in the total simulation time, which was on average 14 min for *Patients 1-10*. The total treatment

time (up until beam on) can be shorter in reality, as there was a delay in the emulator, which prolonged the waiting time between each step. For treatments where seminal vesicles are included in the target, they need to be included as influencers. The user will spend more time on influencer editing, but the total treatment time will still be within an acceptable time frame (15-20 min) for prostate EBRT.

The evaluation of the propagated target size, based on the amount of influencer editing, showed a smaller difference between its volume and the reference target volume, when all influencers or only the prostate influencer were edited moderately or considerably. Adjusting the bladder and rectum influencer only, did not have a large effect on the propagated target. The better volume agreement for the cases when all influencers were edited is most probably solely due to editing of the prostate influencer. For a correct target propagation it is sufficient to focus on the prostate influencer to save time during this step of the workflow. However, if the bladder and rectum influencers were not edited, this could cause an incorrect OAR propagation, as they would be elastically instead of structure based deformed. An incorrect OAR propagation leads to inaccurate calculation of absorbed dose to OAR. To summarise, all influencers, except seminal vesicles (which were excluded), needed to be adjusted for correct target and OAR propagation and dose calculation for a prostate only treatment.

According to studies by *King et. al.* and *Nichol et.al.*, for a conventional EBRT treatment (39 fractions), the prostate gland could increase in size in the beginning and shrink below baseline after the treatment [17],[18]. The analysis of the propagated target volume for *Patient A* and *B*, showed a similar trend. The prostate volume for the first fraction was close to the volume of the reference target, which was expected since no interventions had been done. Thereafter, an increase in the difference for fraction 11 and a relative decrease for fraction 21 was seen. This was not the last clinical treatment fraction, so it cannot be determined whether the prostate size continued shrinking. The trend in volume change between fractions was not observed for *Patients 1-10*.

The majority of the propagated targets for all 12 patients were larger in volume than the reference target. It can be suggested that the enlargement in the target is due to the online adaptive process and not solely due to changes in prostate morphology, since the prostate size does not change in reality as much as suggested by the propagated target. It should also be noted that the patients used for these simulations, were treated by using conventional fractionation. Therefore, the change in their anatomy might not fully correspond to the trend expected for a SBRT treatment.

There was a correlation between influencer prostate volume and propagated target volume, see Figure C.2 in Appendix C. This correlation was due to the fact that the propagated target was created by structure guided deformation based on the prostate influencer. Therefore, an inaccurately adjusted influencer volume will lead to a falsely enlarged target. The inaccu-

racy in prostate influencer adjustment can be due to several factors. The AI-algorithm can be biased for propagating the prostate influencer larger, which can affect the adjustments done by the user, who uses the initial contours as a base. The increase in propagated target size can also be due to changes in bladder and rectum influencers. For example, *Patient 4* who had large difference between the propagated and reference targets, seemed to have large variations in the rectum influencer. Same applies for *Patients 6* and *7*, who had variations in both rectum and bladder, see figure 4.4. The size of the propagated influencers can contribute to the increased volume of the propagated target. Another explanation for inaccurate influencer adjustment can be the CBCT image quality. Due to insufficient soft-tissue contrast, it is hard to see prostate borders on CBCT-images, which is why MR-images are used for target delineation. Target and OAR propagation is also user dependant. A user who is more acquainted with CBCT image quality, will be able to adjust prostate influencer contours more accurately. Hence improve the guidance for the propagation of target. It is also important to know the specific patient's anatomy, as this can be advantageous in influencer and target adjustment.

It was observed that the AI-algorithm propagated the prostate influencer larger in the CC direction. This observation was supported by the analysis of the residual image slice difference between propagated and reference target, which showed larger differences in the CC direction and the AP direction. These observations were in accordance with what was stated in the literature [22]. The difference in the AP direction can be explained by the changes in the rectum size, while the difference in the CC direction can be due to the difficulty in defining the prostate in that direction. For example, *Patient 3* had a good volume agreement between propagated and reference target. However, majority of its propagated targets were extending outside the reference PTV in the AP direction. The same patient had larger variations in the rectum influencer volume, which could have shifted the propagated target position. The residual image slice differences in Figure 4.3 can also be due to enlarged target and not an actual difference in the position. This was observed for *Patients A* and *B* (Figure C.3, Appendix C). The reference target volume and the propagated target volume overlapped, but the latter was larger and hence appeared as shifted when the difference in residual slice was calculated. Fiducial marker migration was observed in a study [18]. Hence, some of the observed position and volume differences can also be due to migration of fiducial markers which were used as a guidance for these evaluations. Migration changes the volume distribution around the markers, leading to differences in the propagated and reference target when they are overlapped. This can be investigated for patients who had large differences in the position, despite of a good volume agreement.

Shifts in target position and size differences are important for SBRT treatments, since high doses are applied. The uncertainties in target and OAR propagation need to be incorporated in the margins. Based on the results for *Patient A* and *B*, the 5 mm isotropic margin was validated during the treatment simulations. A large change to the currently used margin

at Herlev Hospital for prostate cancer was not made due to lack of enough statistics. The position evaluation of the propagated targets for *Patients 1-10* showed that the majority of the propagated targets were within the reference PTV. This implies that the used margins were sufficient and covered for the shifts in position. For the cases when the differences were larger than 5 mm, the reference target was covered by the propagated target and PTV. Using the statistics for the other 10 patients, the margin for oART can be recalculated. In this calculation, uncertainties in sCT should be taken into account. Quality of the sCT is an important factor in dose calculation for the scheduled and adapted plans. During treatment, only the position of high density structures are checked on the sCT and its quality is not evaluated thoroughly. The issues around the sCT were not considered in this project. Another way of optimising CTV-PTV margins further would be to track the intra-fractional changes in the target by incorporating real-time target tracking method to daily oART. By taking into account all the above mentioned factors, the margins for daily oART of prostate cancer can be optimised for maximum target coverage and sparing of OAR. This re-calculation of the margins was not done in this project.

5.2 Dose distribution comparison for oART

A statistically significant difference between the adapted and scheduled plans was seen in CTV and PTV coverage. Most patients benefited from the increased target coverage the adapted plan provided. This was expected based on the volumetric and positional analysis of the propagated targets. Since the propagated target size was generally larger than the reference target, which the scheduled plan is based on, the CTV and PTV coverage was not expected to be as sufficient for the scheduled plan as it was for the adapted. However, the improved coverage with adaptation can be due to an incorrectly enlarged target. As stated in Section 5.1, the volume difference did not follow the trends for conventionally fractionated EBRT stated in literature [17],[18]. If these observed changes in the volume of the propagated target are not due to changes in prostate morphology and that in reality the prostate size did not change significantly, it can be assumed that both plans would have the same performance. If the enlargement in propagated target is incorrect, as suggested in Section 5.1, adaptation can even be a disadvantage. An increase in CTV and consequently in PTV, will lead to irradiation of larger volume of rectum and healthy tissue.

There was no significant difference in the absorbed dose to the rectum. The variation in the dose was larger for the scheduled plan compared to the reference and adapted plans. There were outliers in the adapted plan for the absorbed dose to rectum (Figures 4.5c-4.5e). These were for *Patients 1* and *6*. The higher dose to rectum is probably due to rectum being very close to prostate and adaptation not being able to improve rectum sparing and simultaneously have good target coverage.

The results showed that the benefit with daily adaptation varied between patients. Some

benefited from the use of an adapted plan and others had better constraints fulfillment for the scheduled plan. An example for such cases is shown in Figure 4.6. Both patients' propagated targets differed from their reference targets by less than 5%, so it can be assumed that the dose distribution is not a consequence of an enlarged target. *Patient 1* benefited from adaptation during treatment *fraction 3*, where he had smaller bladder than on the planning CT and larger rectum. *Patient 3*, who did not have a large benefit from adaptation for *fraction 5*, had a much smaller bladder during that fraction than on the planning CT, but the rectum size was similar. Hence, if the patient has large variation from one treatment to another, oART is often beneficial for that patient. Adaptation also has the potential to be beneficial for patients without large variations, since it can allow determination of patient specific margins.

Chapter 6

Conclusion

The results of the study show that the Ethos system can propagate an MR-based target when CT-based influencers are used. The size of the target was generally larger for the 12 test patients, but its shape and position corresponded well with the MR-based target. There was a statistically significant improvement in CTV and PTV coverage for the adapted plan compared to the scheduled plan. However, no significant difference was observed in the dose to rectum. Online adaptive SBRT improved the target coverage and OAR sparing for patients with large variations in the anatomy.

Online adaptive SBRT can be beneficial for more patients, if target propagation is optimized further and CTV-PTV margins are re-calculated taking into account uncertainties introduced during the oART workflow.

Chapter 7

Outlook

The results of this study imply that target propagation needs to be investigated further. To determine whether the observed target enlargement is accurate, a radiologist or an oncologist can evaluate the propagated targets. Additionally, the treatment simulations can be re-done by other users to investigate inter-user variability. The propagation algorithm can be optimised further to avoid incorrect enlargement of the prostate. High-density structures, such as fiducial markers, can be used as a guide for target propagation for cases when soft tissue contrast in CBCTs is insufficient. The workflow can be adapted to allow a gold fiducial marker based registration between CBCT and planning CT images to set the propagated target position. In this way the uncertainties in the target position can be eliminated. The maximum volume variation between reference and propagated targets can also be limited using trends observed in literature.

Furthermore, the quality of the sCT should be investigated and incorporated in the uncertainty estimations. The CTV- PTV margins can be re-calculated based on the statistics from the treatment simulations and the possibility to decrease the margin towards rectum should be investigated to spare rectum for more patients.

Finally, it could be reasonable to initiate a clinical trial to investigate the benefits with online adaptive SBRT of prostate cancer. The major interest of the study would be to study patient-specific outcome and toxicity to OAR.

References

[1] H. O. Adami, D. J. Hunter, P. Lagiou, and L. Mucci, *Textbook of Cancer Epidemiology [Electronic book]*. New York, USA: Oxford University Press, 2 ed., 2018.

[2] Cancerfonden, "Cancerfondsrapporten 2018," tech. rep., Cancerfonden, 2018.

[3] R. Miralbell, S. A. Roberts, E. Zubizarreta, and J. H. Hendry, "Dose-fractionation sensitivity of prostate cancer deduced from radiotherapy outcomes of 5,969 patients in seven international institutional datasets: α/β = 1.4 (0.9–2.2) Gy," *International Journal of Radiation Oncology, Biology, Physics*, vol. 82, no. 1, pp. e17 – e24, 2012.

[4] C. N. Catton, H. Lukka, C.-S. Gu, J. M. Martin, S. Supiot, P. W. Chung, G. S. Bauman, J.-P. Bahary, S. Ahmed, P. Cheung, K. H. Tai, J. S. Wu, M. B. Parliament, T. Tsakiridis, T. B. Corbett, C. Tang, I. S. Dayes, P. Warde, T. K. Craig, J. A. Julian, and M. N. Levine, "Randomized trial of a hypofractionated radiation regimen for the treatment of localized prostate cancer," *Journal of Clinical Oncology*, vol. 35, no. 17, pp. 1884–1890, 2017.

[5] B. E. Hickey, M. L. James, T. Daly, F. Y. Soh, and M. Jeffery, "Hypofractionation for clinically localized prostate cancer," *Cochrane database of systematic reviews*, vol. 9, no. 9, 2019.

[6] P. Verze, T. Cai, and S. Lorenzetti, "The role of the prostate in male fertility, health and disease," *Nature Reviews Urology*, vol. 13, 6 2016.

[7] C. H. Lee, O. Akin-Olugbade, and A. Kirschenbaum, "Overview of prostate anatomy, histology, and pathology," *Endocrinology and Metabolism Clinics of North America*, vol. 40, no. 3, pp. 565 – 575, 2011.

[8] R. Prashanth, "Epidemiology of prostate cancer," *World Journal of Oncology*, vol. 10, no. 2, pp. 63–89, 2019.

[9] Physician Data Query (PDQ) Adult Treatment Editorial Board, "PDQ prostate cancer treatment," *PDQ Cancer Information Summaries [Internet]*, 2020.

[10] W. S. Jr., N. J. Tarbell, and M. Yao, eds., *Clinical Radiation Oncology: Indications, Techniques, and Results [Electronic book]*. Oxford, UK: John Wiley & Sons, 3 ed., 2017.

[11] E. B. Podgorsak, *Radiation Physics for Medical Physicists [Electronic book]*. Switzerland: Springer International Publishing, 3 ed., 2016.

[12] E. Hall, *Radiobiology for the radiologist [Electronic book]*. Philadelphia, USA: Lippincott Williams & Wilkins, 7 ed., 2012.

[13] S. U. Tetar, A. M. Bruynzeel, F. J. Lagerwaard, B. J. Slotman, O. Bohoudi, and M. A. Palacios, "Clinical implementation of magnetic resonance imaging guided adaptive radiotherapy for localized prostate cancer," *Physics and Imaging in Radiation Oncology*, vol. 9, pp. 69–76, 2019.

[14] J. M. Beckta, J. D. Nosrati, and J. B. Yu, "Moderate hypofractionation and stereotactic body radiation therapy in the treatment of prostate cancer," *Urologic Oncology: Seminars and Original Investigations*, vol. 37, no. 9, pp. 619 – 627, 2019.

[15] M. E. Hwang, M. Mayeda, M. Liz, B. Goode-Marshall, L. Gonzalez, C. D. Elliston, C. S. Spina, O. A. Padilla, S. Wenske, and I. Deutsch, "Stereotactic body radiotherapy with periprostatic hydrogel spacer for localized prostate cancer: toxicity profile and early oncologic outcomes," *Radiation Oncology*, vol. 14, no. 136, 2019.

[16] D. J. Sher, R. B. Parikh, S. Mays-Jackson, and R. S. Punglia, "Cost-effectiveness analysis of SBRT versus IMRT for low-risk prostate cancer," *American Journal of Clinical Oncology*, vol. 37, no. 3, p. 215-221, 2014.

[17] B. L. King, W. M. Butler, G. S. Merrick, B. S. Kurko, J. L. Reed, B. C. Murray, and K. E. Wallner, "Electromagnetic transponders indicate prostate size increase followed by decrease during the course of external beam radiation therapy," *International Journal of Radiation Oncology, Biology, Physics*, vol. 79, no. 5, pp. 1350 – 1357, 2011.

[18] A. M. Nichol, K. K. Brock, G. A. Lockwood, D. J. Moseley, T. Rosewall, P. R. Warde, C. N. Catton, and D. A. Jaffray, "A magnetic resonance imaging study of prostate deformation relative to implanted gold fiducial markers," *International Journal of Radiation Oncology,Biology,Physics*, vol. 67, no. 1, pp. 48 – 56, 2007.

[19] A. Gunnlaugsson, E. Kjellén, O. Hagberg, C. Thellenberg-Karlsson, A. Widmark, and P. Nilsson, "Change in prostate volume during extreme hypo-fractionation analysed with MRI," *Radiation Oncology*, vol. 9, no. 22, 2014.

[20] E. M. Quan, L. Xiaoqiang, L. Yupeng, W. Xiaochun, R. J. Kudchadker, J. L. Johnson, D. A. Kuban, A. K. Lee, and Z. Xiaodong, "A comprehensive comparison of IMRT and VMAT plan quality for prostate cancer treatment," *International Journal of Radiation Oncology, Biology and Physics*, vol. 83, no. 4, 2012.

[21] The International Commission on Radiation Units and Measurements (ICRU), "Prescribing, recording, and reporting intensity-modulated photon-beam therapy (IMRT)(ICRU Report 83)," tech. rep., 2010.

[22] R. Levin-Epstein, G. Qiao-Guan, J. E. Juarez, Z. Shen, M. L. Steinberg, D. Ruan, L. Valle, N. G. Nickols, P. A. Kupelian, C. R. King, M. Cao, and A. U. Kishan, "Clinical assessment of prostate displacement and planning target volume margins for stereotactic body radiotherapy of prostate cancer," *Frontiers in Oncology*, vol. 10, 2020.

[23] M. van Herk, P. Remeijer, C. Rasch, and J. V. Lebesque, "The probability of correct target dosage: dose-population histograms for deriving treatment margins in radiotherapy," *International Journal of Radiation Oncology,Biology,Physics*, vol. 47, no. 4, pp. 1121–1135, 2000.

[24] M. J. Ghilezan, D. A. Jaffray, J. H. Siewerdsen, M. Van Herk, A. Shetty, M. B. Sharpe, S. Z. Jafri, F. A. Vicini, R. C. Matter, D. S. Brabbins, and A. A. Martinez, "Prostate gland motion assessed with cine-magnetic resonance imaging (cine-MRI)," *International Journal of Radiation Oncology,Biology,Physics*, vol. 62, no. 2, p. 406-417, 2005.

[25] T. Budiharto, P. Slagmolen, K. Haustermans, F. Maes, S. Junius, J. Verstraete, R. Oyen, J. Hermans, and F. Van den Heuvel, "Intrafractional prostate motion during online image guided intensity-modulated radiotherapy for prostate cancer," *Radiotherapy and Oncology*, vol. 98, no. 2, p. 181-186, 2011.

[26] S. Yartsev and G. Bauman, "Target margins in radiotherapy of prostate cancer," *The British Journal of Radiology*, vol. 89, no. 1067, 2016.

[27] Varian Medical Systems, "Ethos™ therapy AI: Technical Brief," tech. rep., 3 2020.

[28] K. H. Zou, S. K. Warfield, A. Bharatha, C. M. Tempany, M. R. Kaus, S. J. Haker, W. M. Wells, F. A. Jolesz, and R. Kikinis, "Statistical validation of image segmentation quality based on a spatial overlap index," *Academic Radiology*, vol. 11, no. 2, p. 178–189, 2004.

[29] S. U.Tetar, A. M.E.Bruynzeel, F. J.Lagerwaard, B. J.Slotman, O. Bohoudi, and M. A.Palacios, "Clinical implementation of magnetic resonance imaging guided adaptive radiotherapy for localized prostate cancer," *Physics and Imaging in Radiation Oncology*, vol. 9, pp. 69 – 76, 2019.

[30] R. F. Mould, *Introductory medical statistics [Electronic book]*. Institute of Physics Publishing, 3 ed., 1998.

[31] Khan Academy, "Standard deviation: calculating step by step (article)." `https://www.khanacademy.org/math/probability/data-distributions-a1/summarizing-spread-distributions/a/calculating-standard-deviation-step-by-step`.

[32] A. S. Korsager, J. Carl, and L. R. Østergaard, "Comparison of manual and automatic MR-CT registration for radiotherapy of prostate cancer," *Journal of Applied Clinical Medical Physics*, vol. 17, no. 3, pp. 294–303, 2016.

Appendix A

Patient information

Table A.1: Information about the test patients. *Number of clinical fractions* is the number of fractions that the test patients received clinically. The *CBCT fractions* are the fractions from which CBCTs were used in the simulations. The last four columns present the volumes of the reference structures, the target (MR-defined prostate) and the influencers (rectum, bladder and CT-defined prostate).

Patient	*Number of clinical fractions*	*CBCT fractions*	*MR prostate volume [cm^3]*	*Rectum volume [cm^3]*	*Bladder volume [cm^3]*	*CT prostate volume [cm^3]*
A	39	1, 11,21	28.8	23.0	150.6	30.3
B	39	1,11,21	23.3	100.9	146.7	28.3
1	39	1,14,21,28,36	42.1	40.8	243.2	50.8
2	39	1,14,21,28,37	28.6	61.7	96.3	36.2
3	20	1,8,12,16,20	82.7	81.6	254.3	87.7
4	39	7,14,21,28,37	31.2	70.7	139.8	35.2
5	20	1,8,12,16,20	31.0	42.7	299.3	41.5
6	39	1,14,21,28,36	79.2	62.9	313.2	91.3
7	39	1,14,21,28,36	39.5	58.0	133.0	47.1
8	39	7,14,21,28,36	20.4	47.9	149.6	26.5
9	20	2,8,12,16,20	34.2	62.7	243.0	43.9
10	20	1,8,12,16,20	54.5	47.6	239.5	63.4

Table A.2: The average time spent on editing specific influencers for *Patients A* and *B*. For *Patients 1-10*, both the average time spent on editing all influencers and the total simulation time are presented.

Patient	*Influencer edited*	*Average influencer editing time [min]*	*Average total simulation time [min]*
A&B	Prostate moderate	2.60	-
A&B	Prostate considerable	3.40	-
A&B	Bladder	2.10	-
A&B	Seminal vesicles	2.40	-
A&B	Rectum	2.30	-
1	All	8.60	13.60
2	All	13.40	19.40
3	All	9.30	15.90
4	All	8.00	12.90
5	All	7.90	12.60
6	All	10.50	17.10
7	All	7.60	12.80
8	All	5.80	11.80
9	All	7.90	13.30
10	All	7.00	11.70

Appendix B

Data distribution

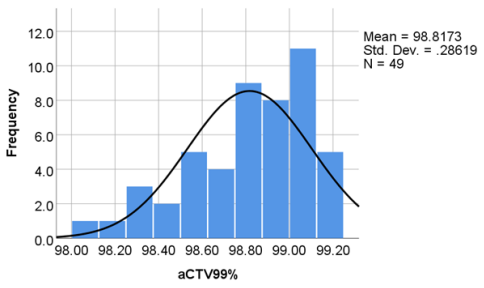

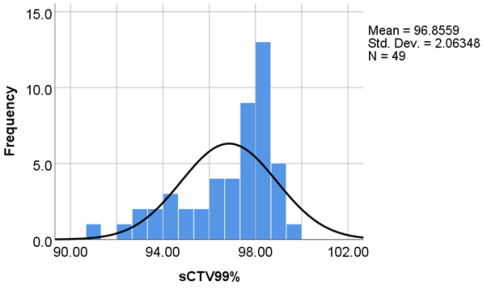

(a) Absorbed dose to 99% of CTV volume, measured in percentage.

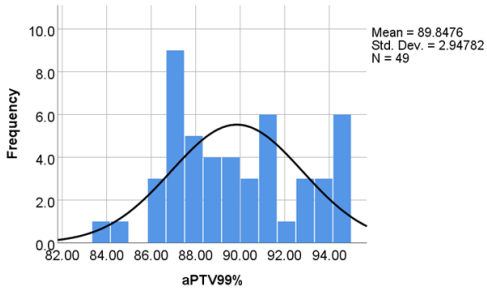

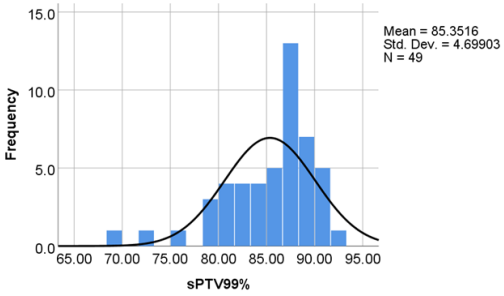

(b) Absorbed dose to 99% of PTV volume, measured in percentage.

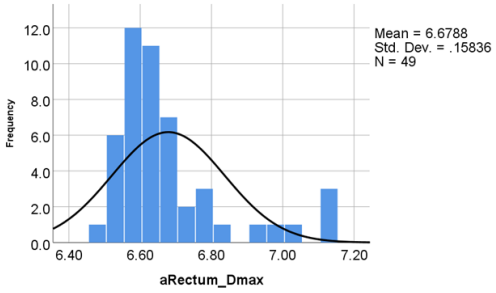

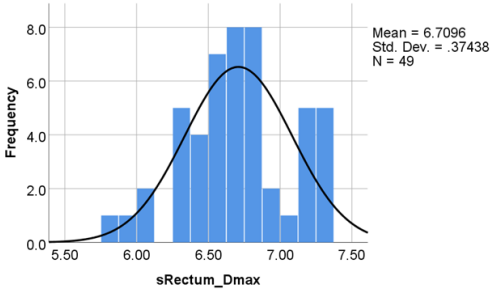

(c) Maximum absorbed dose to rectum, measured in Gy.

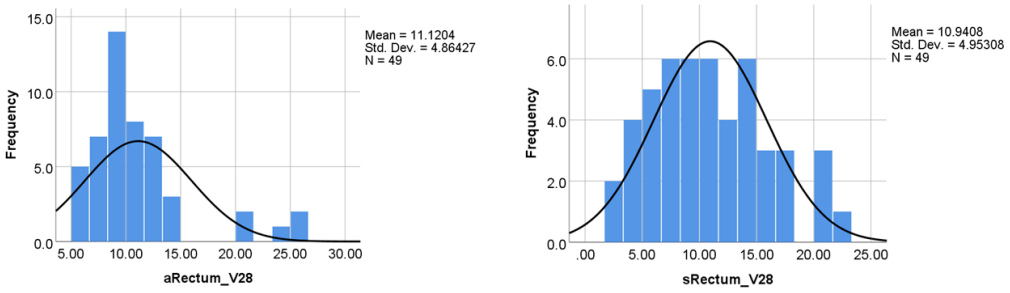

(d) Rectum volume that receives 28 Gy, measured in percentage.

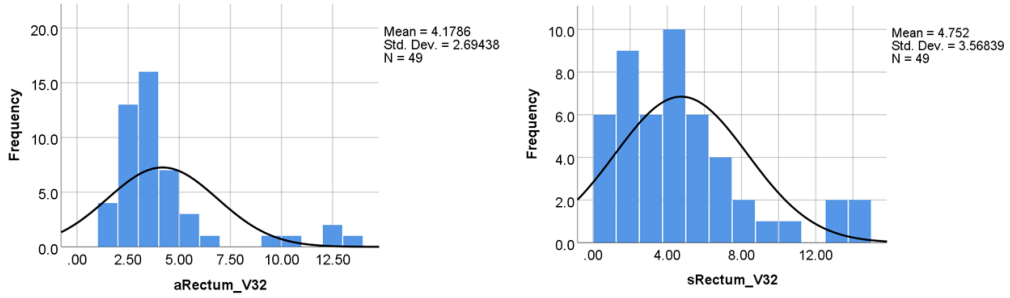

(e) Rectum volume that receives 32 Gy, measured in percentage.

Figure B.1: Data distribution of the parameters stated above. The histograms to the right represent the distribution for the scheduled plans and the histograms to the left- for the adapted plans.

Appendix C

Influencer and target propagation

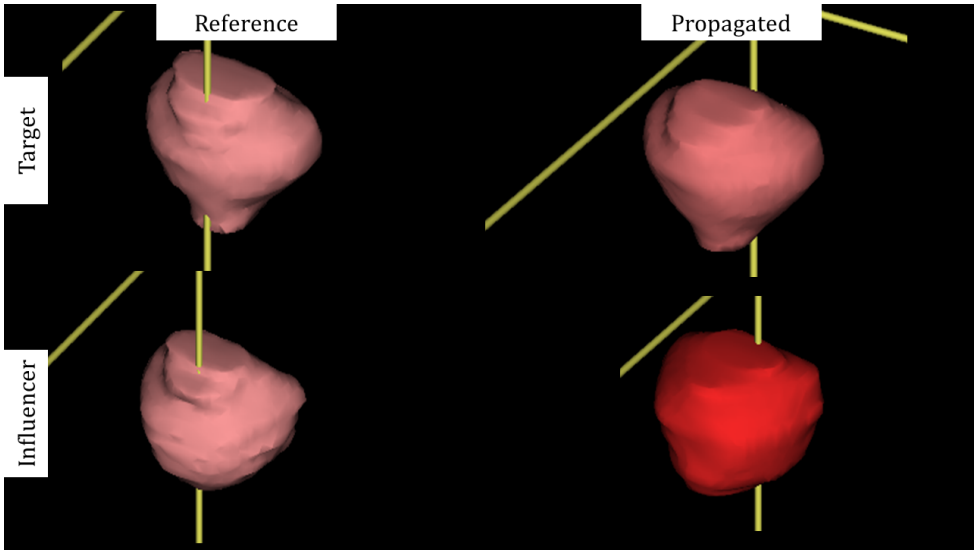

(a) Patient 4, who had the largest difference between propagated and reference target.

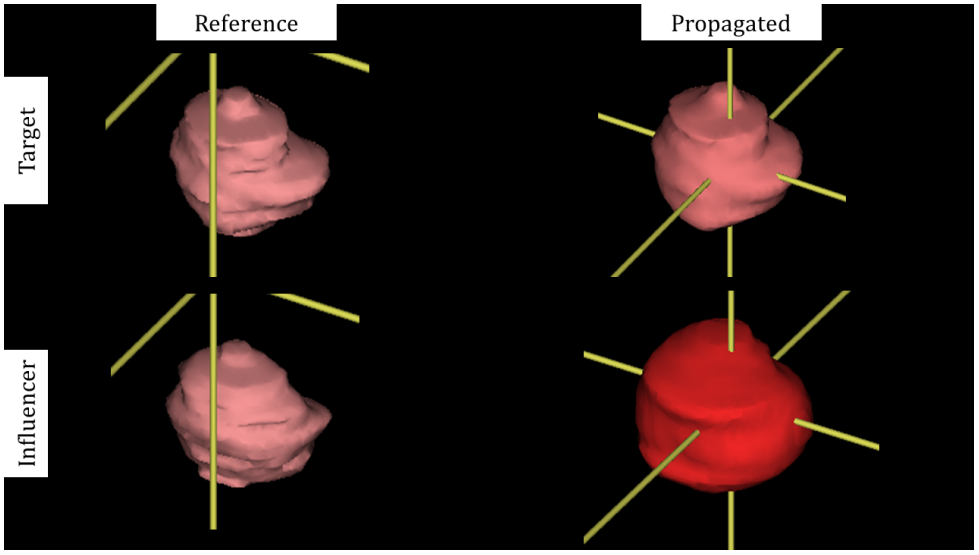

(b) Patient 9, who had the smallest difference between propagated and reference target.

Figure C.1: A three dimensional view of the reference and propagated MR-based prostate targets and CT-based prostate influencers.

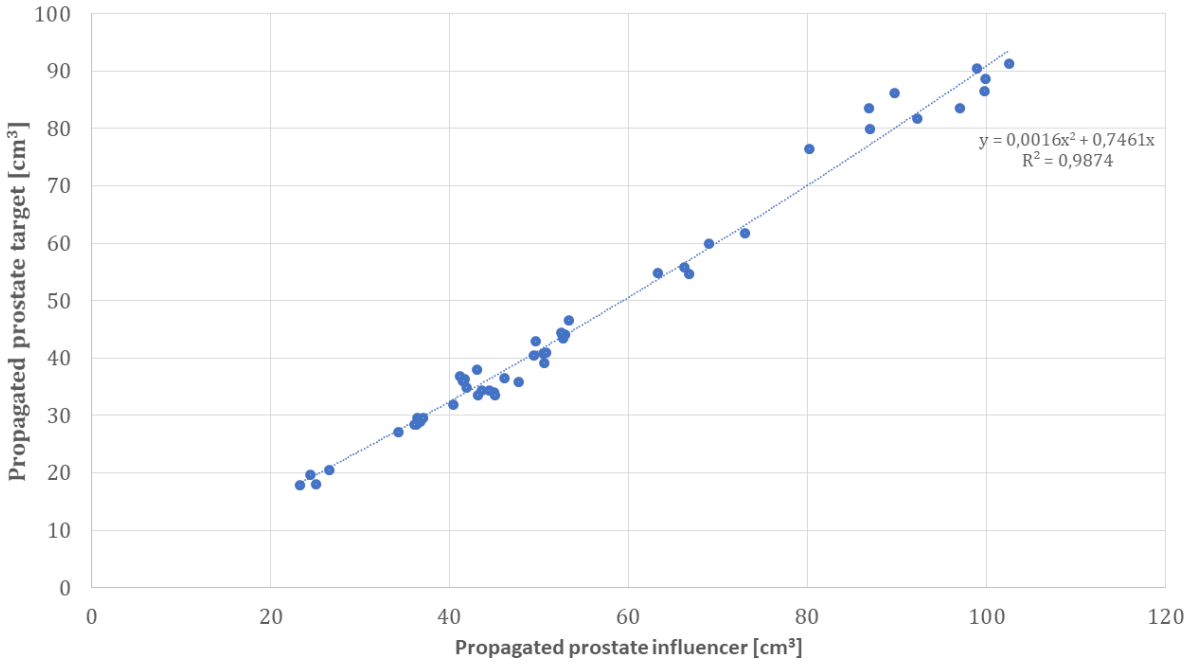

Figure C.2: Volume of propagated prostate target plotted as a function of propagated prostate influencer volume. There is a strong correlation between these parameters.

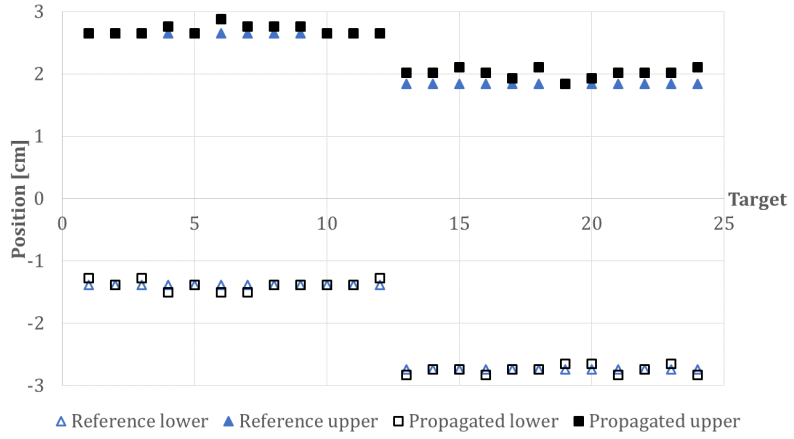

(a) Left-right direction

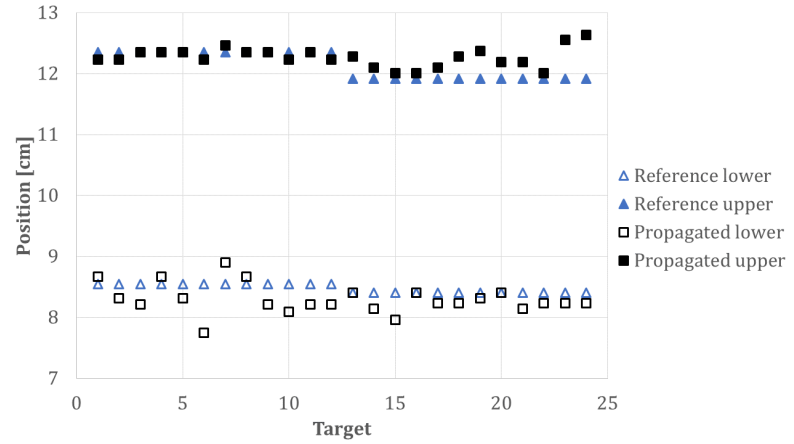

(b) Anterior-posterior direction

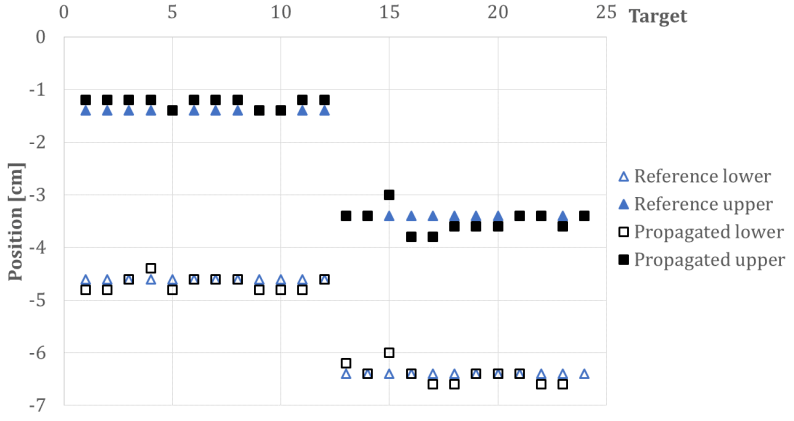

(c) Cranio-caudal direction

Figure C.3: The image slices, where the reference and propagated targets begin and end in each direction. The data is for *Patients A* and *B*.

Appendix D

Dose distribution

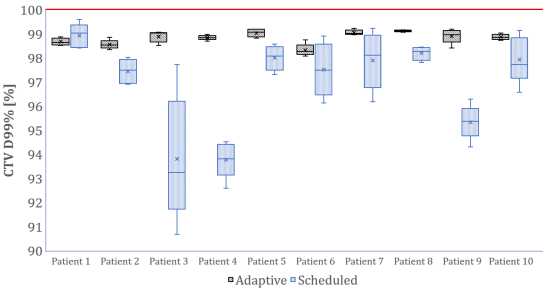

(a) Absorbed dose to 99% of CTV volume.

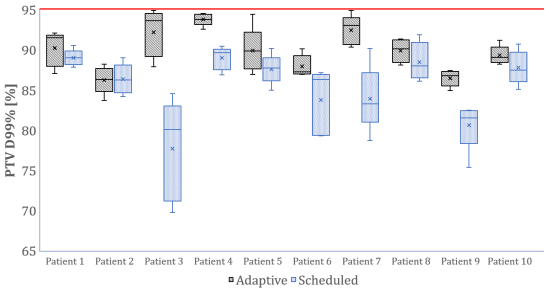

(b) Absorbed dose to 99% of PTV volume.

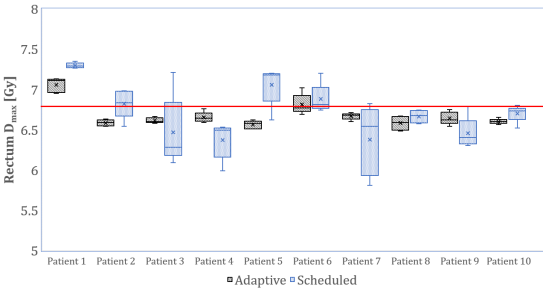

(c) Maximum absorbed dose to rectum.

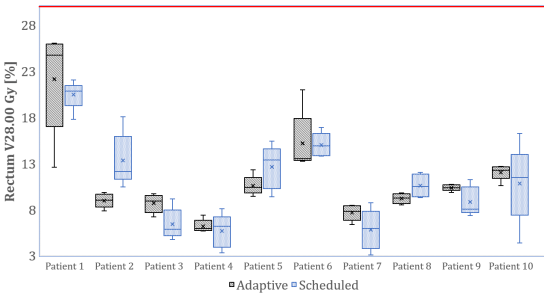

(d) Rectum volume that receives 28 Gy.

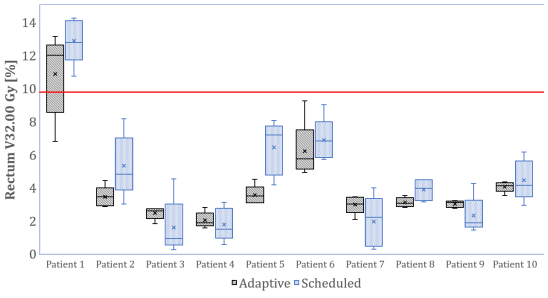

(e) Rectum volume that receives 32 Gy.

Figure D.1: Box and whisker plots comparing absorbed dose to CTV, PTV and rectum for scheduled and adapted plans for all fractions of each patient. The red line represents the treatment planning constraint.